[American Journal of Science, Vol. 303, September, 2003, P. 622–665]

THE SAGHAND REGION, CENTRAL IRAN: U-Pb GEOCHRONOLOGY, PETROGENESIS AND IMPLICATIONS FOR GONDWANA TECTONICS

JAHANDAR RAMEZANI* and ROBERT D. TUCKER

Department of Earth and Planetary Sciences, Washington University, St. Louis, Missouri 63130

ABSTRACT. The Saghand area of East-Central Iran exposes rocks that comprise the substratum of the Central Iranian continental terrane, as part of the larger Alpine-Himalayan orogenic system. Our new U-Pb ages and geochemical data from the magmatic, metamorphic and siliciclastic rocks of the Saghand area unravel three main episodes of orogenic activity in the latest Neoproterozoic-Early Cambrian, the Late Triassic, and the Eocene. Geologic events in the oldest episode include in chronological order, low- to medium-grade metamorphism, calc-alkaline plutonism, rhyolitic to andesitic volcanism, and widespread trondhjemite emplacement, from 547 Ma to 525 Ma. The Late Triassic event (approximately 220-213 Ma) is characterized by the emplacement of granite-tonalite plutons. The extensive, high-grade metamorphic rocks, migmatites and post-kinematic intrusions of Eocene age (47-44 Ma) occur in a distinct domain, in the western part of the Saghand area. These rocks previously were thought to represent the Precambrian basement of the Central Iranian Terrane.

The terminal Neoproterozoic-Early Cambrian orogeny in central Iran was related to a broad-scale magmatic arc that developed along the Proto-Tethyan margin of the Gondwanaland supercontinent. The fragmented remains of that margin occur as displaced terranes, including the Central Iranian Terrane, now embedded within the Alpine-Himalayan orogenic system. The newly recognized Late Triassic intrusions of the Saghand area are indicative of a tectonomagmatic episode of possible collisional nature, in accord with the previously identified Early Kimmerian (Cimmerian) event in the region. The extensive Eocene metamorphic and magmatic activities correspond to the early Alpine Orogeny, which resulted from the convergence between Arabian and Eurasian plates, and the Cenozoic closure of the Tethys oceanic tract(s) by subduction.

INTRODUCTION

The Central Iranian Terrane is an approximately 2300 km^2 region of moderate relief surrounded by fold-and-thrust belts, within the Alpine-Himalayan orogenic system of western Asia (fig.1). It is located in the broad segment between two impingement points (syntaxes) of the Alpine-Himalayan system; the Turkish syntax to the west and the Pamir syntax to the east. The Alborz and Kopeh-Dagh ranges to the north, Zagros and Makran ranges to the west and south, and the East Iran Ranges to the east border this terrane. Being situated to the northeast of the Zagros-Makran Neo-Tethyan suture and its sub-parallel Cenozoic magmatic arc (fig.1), the Central Iranian Terrane is an area of continuous continental deformation in response to the ongoing convergence between the Arabian (Gondwanan) and Turan (Eurasian) plates.

The concept of a distinct, fault-bounded "Central and East Iranian Microcontinent", which was once encircled by Red Sea type oceanic tracts represented now by strips of ophiolitic rocks, was first introduced by Takin (1972). Early comparative stratigraphic studies in the Zagros Ranges of southern Iran (fig.1) had revealed its geologic setting as the passive continental margin of the Arabian Plate (see for example, Stöcklin, 1968). The overall uniformity of the Eocambrian (late Neoprotero-

*Present address: Earth, Atmospheric and Planetary Sciences, Massachusetts Institute of Technology, Bldg. 54-1020, Cambridge, Massachusetts 02139; ramezani@mit.edu

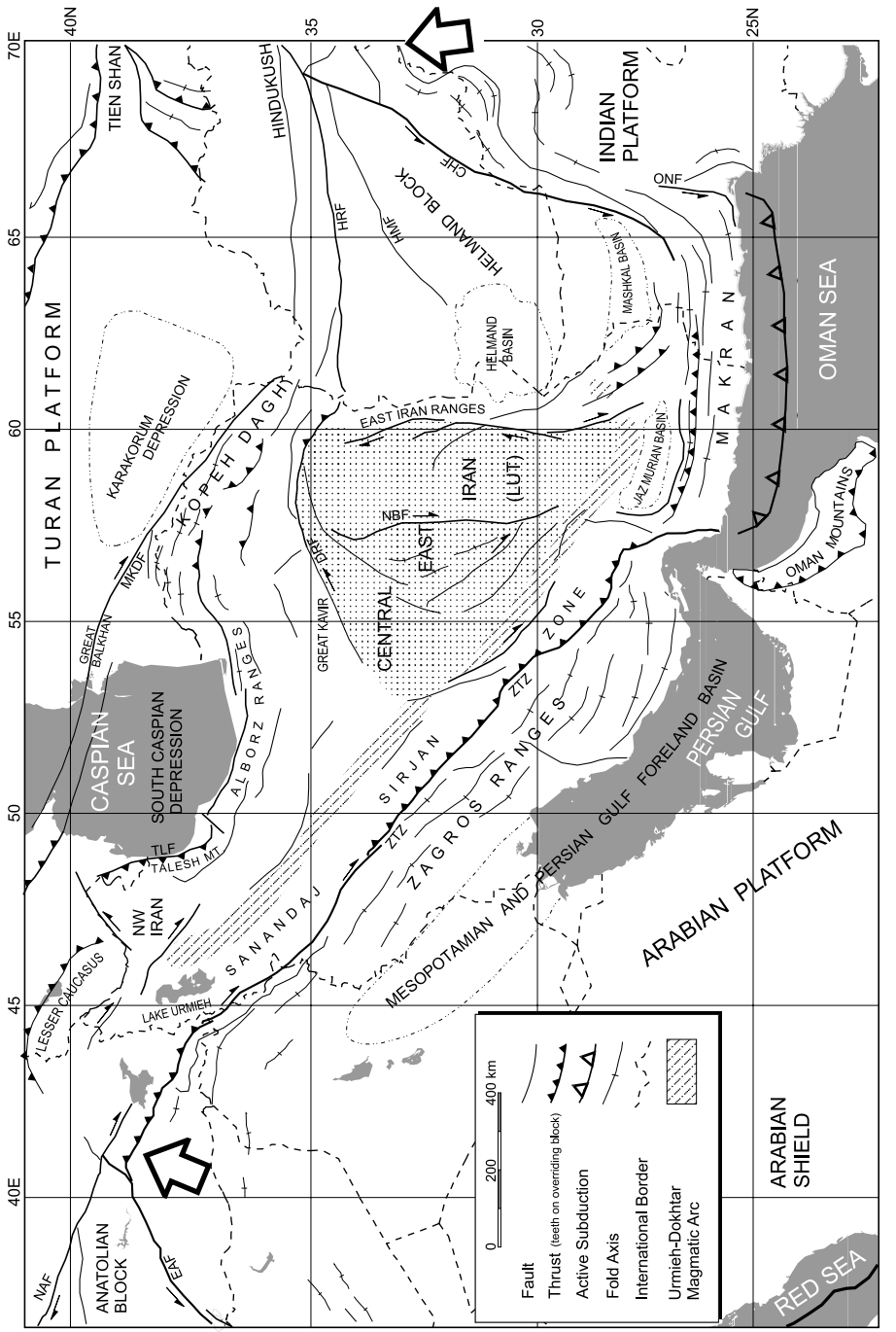

Fig. 1. Simplified structural map of Iran and adjacent regions (compiled from Berberian, 1981; Jackson and McKenzie, 1984; Alavi, 1991). Large arrows illustrate the syntaxes of the Alpine-Himalayan Orogenic System: 1 = Turkish Syntax, 2 = Pamir-Hindukush Syntax. CHF = Chaman Fault, DRF = Doruneh Fault, EAF = Eastern Anatolian Fault, HRF = Herat Fault, HMF = Helmand Fault, MKDF = Main Kopeh-Dagh Fault, NAF North Anatolian Fault, NBF = Nayband Fault, ONF = Ornach Nal Fault, ZTZ = Zagros Thrust Zone.

zoic) and Paleozoic platform strata that covered the Zagros, Central Iran (*sensu lato*) and the Main Alborz provinces led to the predominant notion that all of these regions were once part of the undivided Paleozoic Arabian-Iranian platform of the Gondwanaland supercontinent (Stöcklin, 1968, 1974; Crawford, 1972). By analogy to the Arabian shield and platform, continental crust of late Precambrian age was believed to underlie both Zagros and central Iran. Nevertheless, neither the sparse Rb-Sr isochron data from the central Iranian crystalline rocks (Crawford, 1977) nor the Pb-Pb isochron ages of lead orebodies in central Iran (Huckriede and others, 1962) provided conclusive evidence for the presence of a Precambrian crust in this region. These data rendered the true age and origin of the continental crust in central Iran a matter of debate for nearly four decades. The primary objective of our study was to furnish accurate age constraints on the orogenic episode(s) that governed the formation and later tectonic evolution of the Central Iranian Terrane.

The Central Iranian Terrane consists, from east to west, of three major crustal domains: the Lut Block, Tabas Block and the Yazd Block (see for example, Alavi, 1991). These blocks are separated by a series of intersecting regional-scale faults (fig. 2). Although the stratified cover rocks are largely correlatable among different blocks, locally significant facies and/or thickness variations occur across the domain boundaries. Each block features a particular overall deformation style and pattern of recent seismicity, distinguishable from those in the adjacent domains (Berberian, 1981). The Tabas and Yazd blocks are separated by a nearly 600 kilometer long, arcuate and structurally complex belt composed of variably deformed and fault-bound supracrustal rocks. This belt is herein named the Kashmar-Kerman Tectonic Zone, after the towns of Kashmar and Kerman located at the opposite extremities of the belt (fig. 2). The Kashmar-Kerman Tectonic Zone provides remarkable exposures of the deeper sections of the Central Iranian platform strata, among which the late Neoproterozoic and lower Paleozoic rocks are abundant. Interestingly, the type localities of all of the "Precambrian" to Carboniferous formations in greater central Iran (Stöcklin and Setudehnia, 1977) have been selected from within this relatively narrow belt. The crystalline rocks that underlie the above formations have been uplifted and widely exposed in the vicinity of the town of Saghand, the area of this study (fig. 2).

We report here the first high-precision U-Pb concordia ages, in conjunction with major and trace element data, from the magmatic and metamorphic rocks of the Saghand region. The implications of the new age and petrochemical results for the tectonic evolution of the central Iranian region are discussed. The paleogeographic position of central Iran with respect to the Gondwanan continents is reviewed and correlations are made with rocks of comparable age and settings in adjacent regions.

LITHOSTRATIGRAPHIC FRAMEWORK OF THE SAGHAND REGION

The Kashmar-Kerman Tectonic Zone closely follows the trends of the predominant fault structures of the Central Iranian Terrane (fig. 2), many of which are seismically active or were active in the near past. Three first-order fault systems are identified within the Central Iranian Terrane: the north-trending system (such as Nayband and Nehbandan faults), northeast system (such as Poshteh-Badam and Kalmard faults) and the northwest system (such as Kuhbanan and Rafsanjan faults). The northeast and northwest systems dominate the western half of the terrane which also includes the Kashmar-Kerman Tectonic Zone. A combination of strike-slip (right-lateral) and reverse (thrust) movements associated with these faults has generated a complex pattern of regional deformation involving crustal shortening, horizontal block rotation and localized uplift (Jackson and McKenzie, 1984). The Saghand region, in particular, is situated at the intersection of the northeast and northwest fault systems (fig. 2), where the most extensive documented outcrops of basement rocks in central Iran are exposed.

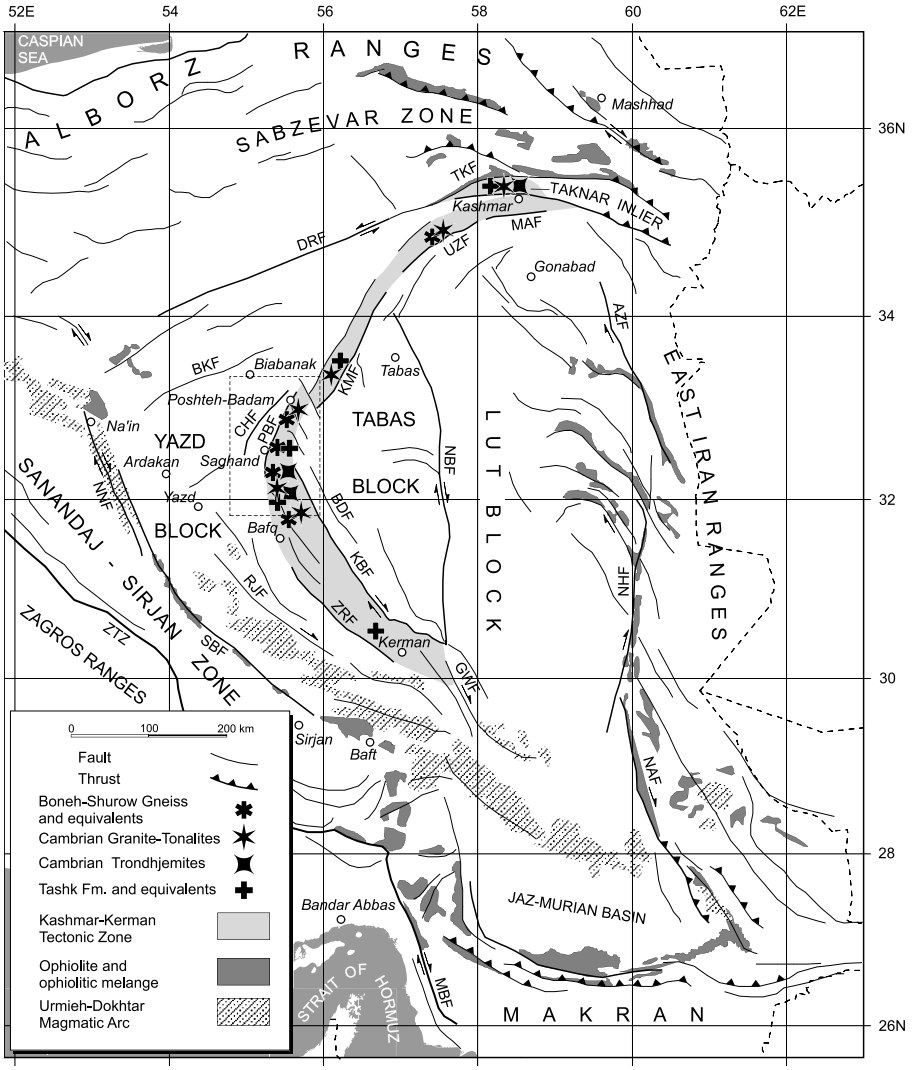

Fig. 2. The structural map of Central-East Iran and its constituent crustal blocks (compiled from Berberian, 1981; Jackson and McKenzie, 1984; Lindenberg and others, 1984; Haghipour and Aghanabati, 1989; Alavi, 1991). Dashed line delineates the study area (fig. 3). Symbols illustrate the distribution of Late-Neoproterozoic to Cambrian rocks throughout the Kashmar-Kerman Tectonic Zone. AZF = Abiz Fault; BDF = Behabad Fault, BKF = Biabanak Fault, CHF = Chapedony Fault, DRF = Doruneh Fault, GWF = Gowk Fault, KBF = Kuhbanan Fault, KMF = Kalmard Fault, MAF = Mehdiabad Fault, MBF = Minab Fault, NAF = Nostratabad Fault, NHF = Nehbandan Fault, NNF = Na'in Fault, RJF = Rafsanjan Fault, SBF = Shahre-Babak Fault, TKF = Taknar Fault, UZF = Uzbak-Kuh Fault, ZRF = Zarand Fault, ZTZ = Zagros Thrust Zone.

The pre-Neogene rocks of the Saghand region are best categorized in terms of three mutually distinct, roughly NNE-trending, "lithotectonic domains" (Ramezani, ms, 1997), bordered from east to west by the Poshteh-Badam Fault, Neybaz-Chatak Fault and the Chapedony Fault, respectively (fig. 3). Rocks of the Eastern Lithotectonic Domain range from lower-amphibolite-facies gneisses (Boneh-Shurow Complex) to virtually unmetamorphosed sedimentary rocks, whereas the Western Lithotectonic

Domain is dominated by high-grade gray gneisses and migmatites (Chapedony Complex). Rocks of the Central Lithotectonic Domain include a variety of metamorphic rocks (Poshteh-Badam Complex) and igneous plutons by and large different from those in the other two domains. Each lithotectonic domain contains a suite of plutonic rocks of distinct age distribution that ranges in lithology from granite to quartz-diorite and, locally, diorite.

The lithostratigraphy of the Saghand region was initially laid out in the context of the geologic quadrangle maps of Ardekan (Valeh and Haghipour, 1970) and Biabanak-Bafq (Haghipour and Pelissier, 1977), published by the Geological Survey of Iran. The stratigraphic subdivisions and nomenclature used herein are primarily those established by those workers, along with revisions, modifications and additions that resulted from our investigations. Detailed descriptions of the corresponding lithostratigraphic units are listed in appendix A.

Haghipour and Pelissier (1977) and Haghipour (1977a, b) classified the mapped igneous intrusions in the Saghand region into five separate groups, based on their lithostratigraphic interpretations. These include the diorite-tonalite (d), granodiorite (gd) and granite (g1) intrusions of Precambrian age, light-colored granite (g2) of late Precambrian (Eocambrian) age and the pink granite (g3) of Mesozoic age. We have substantially revised the above classification in order to accommodate new field and isotopic-age results. Our recommended classification, along with descriptions of the representative plutonic rocks, is given in appendix B.

Eastern Lithotectonic Domain

The Eastern Lithotectonic Domain is the widest of the three-fold domains of the Saghand region. It terminates sharply to the west against the NNE-trending Poshteh-Badam Fault (fig. 3), whereas no major discontinuity is detected across its eastern boundary with the adjacent Tabas Block. The pre-Neogene rocks of the Eastern Domain crop out along a number of roughly WNW-trending mountain ridges (for example, Zamanabad and Boneh-Shurow Mountains) in accord with the northwest structural system of central Iran. These ridges are separated by sub-parallel intermountain depressions filled with Neogene-Quaternary continental deposits.

The main rock units of the Eastern Domain are the Boneh-Shurow Complex, Tashk Formation, the Cambrian Volcano-Sedimentary Unit (appendix A), and a variety of plutonic and shallow intrusive rocks (fig. 3). The most important of these igneous intrusions are the Ariz Granodiorite, Polo Mountian Granodiorite, Zarigan Leucogranite, Douzakh-Darreh Leucogranite and Sefid Granite (appendix B).

Boneh-Shurow Complex.—The Boneh-Shurow Complex (Haghipour and Pelissier, 1977) is the most widely exposed metamorphic unit of the Eastern Domain with ridge-forming outcrops directly adjacent to, and to the east of, the Poshteh-Badam Fault. It exhibits a distinct metamorphic layering composed of an alternation of pink quartzofeldspathic gneisses, greenish-gray mica-schists and dark-colored amphibolites. (see appendix A for detailed rock descriptions). Other subordinate, but important, constituents of the Boneh-Shurow Complex are dolomitic marble interlayers and late-stage, mafic-intermediate magmatic intrusions (for example, diabase dikes) of limited volume.

The predominant mineral assemblages of the Boneh-Shurow schists together with the presence of epidote (and/or clinozoisite) and garnet in many of the Boneh-Shurow rocks are indicative of a lower amphibolite (epidote-amphibolite) metamorphic facies. A protolith of semi-pelitic composition is most consistent with the observed mineralogy of the schists. In contrast, a magmatic (granitic) precursor is proposed for the Boneh-Shurow quartzofeldspathic gneisses based on the occurrence of cross-

hatched (and locally perthitic) microcline and compositionally zoned plagioclase porphyroclasts, together with the total absence of metapelitic aluminosilicates (for example Al_2SiO_2 group minerals and staurolite) in these rocks.

Field and petrologic evidence suggest that the bulk of the Boneh-Shurow Complex must have formed by emplacement of granitic intrusions (sills) into a stratified, predominantly siliciclastic-argillaceous sequence with local mafic volcanic-tuffaceous intervals. The entire complex was subsequently metamorphosed to the lower-amphibolite facies. The late-stage, intermediate to mafic intrusions of the complex apparently did not experience the medium-grade metamorphism and deformation of their host rocks and, hence, must have been post-peak metamorphic.

Tashk Formation.—The well-stratified sequence of weakly metamorphosed, sedimentary and volcanic/volcaniclastic rocks that occur to the east of, and sub-parallel to, the Boneh-Shurow Complex (fig. 3) is known as the Tashk Formation (Haghipour and Pelissier, 1977). The exposed section of the formation in its type locality at Tashk Mountain is estimated to reach 2000 meters. The bulk of the Tashk Formation consists of dark greenish-gray graywackes locally interbedded with arkosic arenites, argillites, tuffaceous deposits and newly identified interlayers of basaltic lava.

The contacts of the Tashk Formation with the Boneh-Shurow Complex, where adequately exposed, are (thrust) faults. Haghipour and Pelissier (1977) inferred a conformable contact between the two units defined by a series of dolomitic marble layers, which they termed the "marble key bed". Our field observations, however, reveal that the marble beds for the most part occur *within* the Boneh-Shurow Complex and do not signify a stratigraphic boundary.

Tashk Formation reflects extensive, terrigenous sedimentation, similar to that in a marginal, outer shelf/slope environment, in the proximity of active volcanic centers. The albite-epidote-actinolite (± chlorite) assemblage of the Tashk metabasalts is characteristic of the greenschist metamorphic facies.

Cambrian Volcano-Sedimentary Unit.—The Cambrian Volcano-Sedimentary Unit (CVSU, Ramezani, ms, 1997) refers to an interlayered sequence of largely unmetamorphosed, intermediate to felsic volcanic rocks, dolomitic limestones and minor gypsum beds, which are largely exposed in the southern portions of the Saghand region. Its outcrops are widespread on both sides of the Poshteh-Badam Fault (fig. 3), with the most complete sections exposed in the Douzakh-Darreh and Zarigan areas of the Eastern Domain. The CVSU and its stratigraphic equivalents throughout central Iran have been collectively classified under "Infracambrian" by previous workers (see for example Stöcklin, 1968; Haghipour and Pelissier, 1977). However, our geochronologic results clearly indicate an Early Cambrian age for the volcanic components of this unit (see below).

The CVSU generally overlies the clastic sedimentary rocks of the Tashk Formation, although their contacts are generally obscured by deformation, granite intrusion and/or hydrothermal alteration. In one isolated location (Douzakh-Darreh Mountain), however, the Tashk-CVSU contact can be characterized as a disconformity. The carbonates of the CVSU unconformably underlie the lower Cambrian red sandstones and conglomerates (Lalun or Dahu Formation) in the Zarigan area as well as in the Bafq region to the south of our study area (Förster and Jafarzadeh, 1994).

Sarkuh Complex.—The Sarkuh Complex (Haghipour, 1977a) is an intercalated sequence of metapelitic rocks and marbles that is exposed exclusively in the Sarkuh Mountain, northeast of Zarigan (fig. 3). The metapelites comprise a variety of mica-schists, including coarse-grained garnet-muscovite-schists and porphyroblastic (andalusite-) biotite-schists with an upper amphibolite metamorphic facies. Prior to the discovery of upper Cambrian fossils in the marbles (Hushmandzadeh, personal

communication, 1996), the Sarkuh Complex was described as a Precambrian metamorphic unit. The contacts of the complex, where exposed, are thrust faults.

Ariz and Polo-Mountain Granodiorites.—The Ariz and Polo-Mountain plutons are both composite igneous intrusions with compositions ranging from tonalite (or quartz-diorite) to granite. The Ariz Granodiorite intrudes the volcanic rocks of the Tashk Formation to the east of the Ariz Mountain, in the southern part of the Saghand region (fig. 3). It appears to have been itself cut by the Zarigan intrusion. Outcrops of the Polo-Mountain Granodiorite are exposed to the east of the town of Poshteh-Badam, where it is emplaced into the Tashk Formation (fig. 3). Smaller intrusive bodies similar in lithology to the Ariz and Polo-Mountain Granodiorites are exposed in a number of locations throughout the Eastern Domain (for example, Douzakh-Darreh area). These intrusions were collectively included in the Precambrian "d" unit of Haghipour and Pelissier (1977).

Zarigan Leucogranite.—The Zarigan intrusion (Haghipour and Pelissier, 1977) is the largest intrusive body exposed in the Saghand region. It underlies two broad, low-relief areas to the east of the Poshte-Sorkh Mountain and further south, to the west of the Zarigan Mountain (fig. 3). Zarigan intrusion is emplaced into the Tashk Formation and the CVSU, and cuts the Ariz Granodiorite. Haghipour and Pelissier (1977) grouped this and lithologically similar, but smaller intrusive bodies in the area (for example Douzakh-Darreh intrusion) under their late Infracambrian "g2" unit.

The Zarigan intrusion is a shallow-level, leucocratic body that ranges in facies from a typical medium-crystalline granite to a subextrusive granite-porphyry. It has the general textural and mineralogical characteristics of low-pressure, hypersolvus granites. Interstitial grains, blobs and veinlets of hematite occur in association with the intrusion, which locally reach economic proportions.

Chemical analyses indicate that the petrographically nondescript feldspar in the Zarigan leucogranite is strongly sodic (albitic) and that the rock should be more accurately classified as a tonalite or trondhjemite, rather than granite. Nonetheless, for the sake of conventionality, the term leucogranite is retained for the Zarigan and related intrusions throughout the Eastern Domain.

The intrusion is typically associated with swarms of mafic (diabase) dikes, many of which exhibit transitional contacts (characterized by clusters of mafic clots) with their host leucogranite. These suggest that the dike intrusion must have been syn- to late-magmatic with respect to the timing of leucogranite crystallization.

Blocks and fragments of country rocks are abundant within the Zarigan intrusion, which may locally reach outcrop dimensions. In the Zarigan Mountain area, two types of enclaves are common; the dark-greenish slaty rocks, and bodies of an extremely sturdy, buff, carbonaceous rock. These enclaves are interpreted to have originated from the Tashk Formation and the CVSU, respectively.

Douzakh-Darreh Leucogranite and Sefid Granite.—An intrusion of medium- to fine-grained leucogranite and its associated mafic (to intermediate) dikes has been emplaced into the Tashk Formation and the CVSU, to the north of the Douzakh-Darreh Mountain (fig. 3). This shallow-level intrusion is notably similar in composition and facies to the Zarigan intrusion which is located about 30 kilometers to its south and west. The country rocks in the vicinity of the Douzakh-Darreh Leucogranite have undergone extensive hydrothermal alteration of argillic (sericite-kaolinite) to advanced argillic (pyrophyllite) types. These rocks have been the subject of exploration for Fe, REE and U ores.

The Sefid (Persian for white) Granite is a coarse-crystalline leucocratic granite that has intruded the Tashk Formation at the Sefid Mountain, to the east of the town of Poshteh-Badam (fig. 3). It has by and large a similar mineralogy to that of the Zarigan Leucogranite, though with different modal abundances. The Sefid Granite also lacks

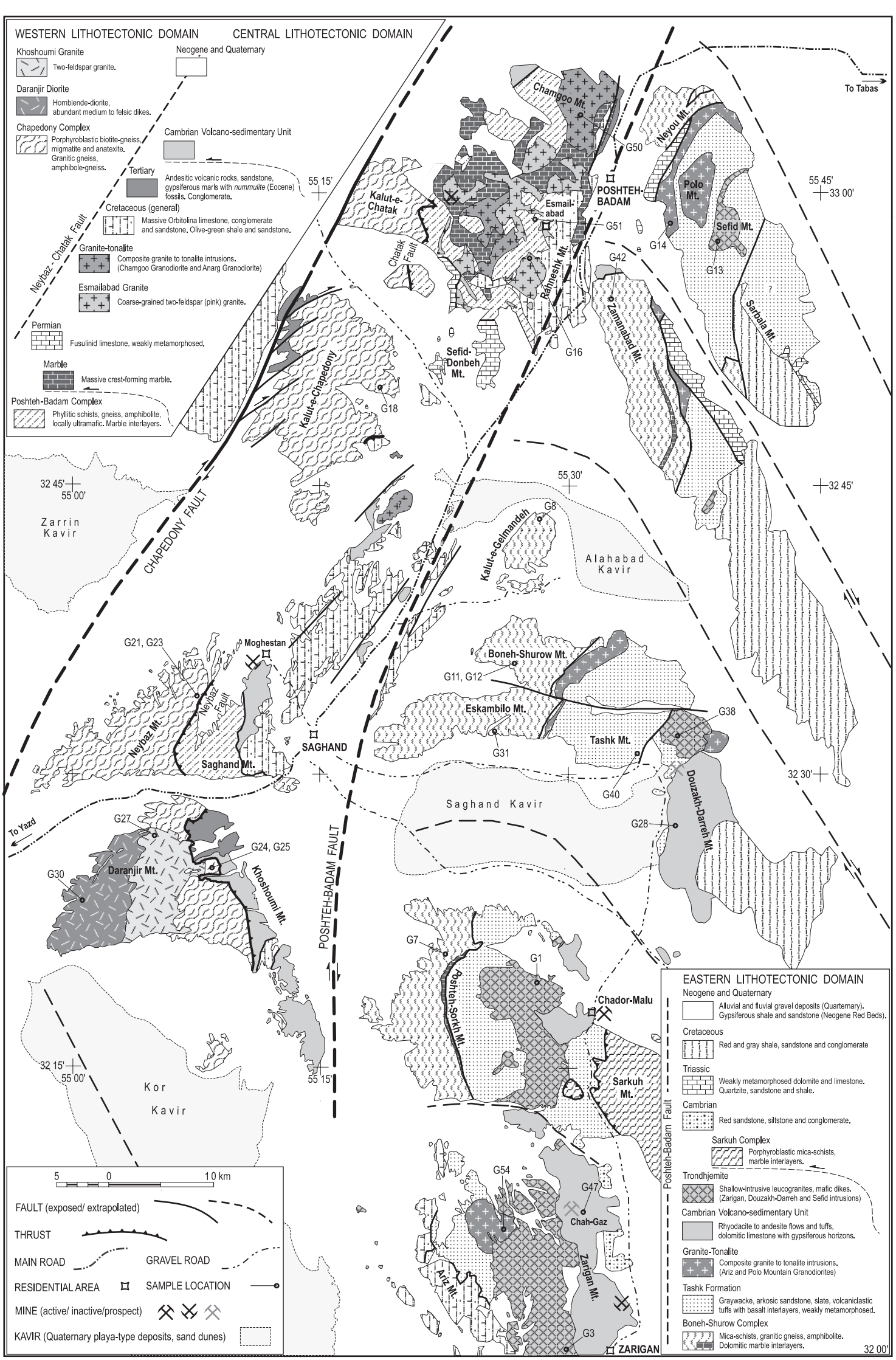

Fig. 3. Geologic map of the Saghand area (modified after Haghipour, 1977a, b) with locations of the dated rocks.

the shallow-level, subextrusive facies of the Zarigan Leucogranite. It was assigned by Haghipour and Pelissier (1977) to the Precambrian "g1" intrusive unit.

Central Lithotectonic Domain

The Central Lithotectonic Domain, with a maximum surface width of approximately 17 kilometers, is a zone of extensive faulting and thrust displacement which is bounded to the east and west by the Poshteh-Badam Fault and the Neybaz-Chatak Fault, respectively (fig. 3). This domain is host to the medium-grade metamorphic rocks of the Poshteh-Badam Complex, as well as several granitic to tonalitic intrusions (Esmailabad, Chamgoo and Anarg intrusions), mainly in its northern part. Segments of the Cambrian Volcano-Sedimentary Unit that occur in this domain are likely to be allochthonous.

Poshteh-Badam Complex.—The diverse assemblage of mainly dark-colored, medium-grade, metamorphic rocks that are exposed to the west of the Poshteh-Badam Fault is known as the Poshteh-Badam Complex (Haghipour and Pelissier, 1977). The main body of the complex in the northern part of the Central Domain is thrust over the high-grade rocks of the Chapedony Complex along the Chatak Fault. A variable association of greenstones, schists, gneisses, amphibolites and marbles comprises the bulk of the Poshteh-Badam Complex. The complex is severely disrupted as the result of thrusting and by the intrusion of granitoid plutons, such that the dispersed outcrops of the complex generally lack continuity.

In addition to the intercalated dolomitic marble layers within the Poshteh-Badam Complex, there are massive crystalline marble sheets that form many crests and hilltops in the northern part of the Central Domain. Close field examinations indicate that the latter are almost invariably in thrust contact with the rocks (for example, greenstones) of the Poshteh-Badam Complex and, therefore, should be considered as a separate lithologic unit (see Marble Thrust Sheets in appendix A).

The rocks of the Poshteh-Badam Complex share many lithologic and facies similarities with those of the Boneh-Shurow Complex in the Eastern Domain. By analogy, a general lower-amphibolite metamorphic facies can be extrapolated for the Poshteh-Badam Complex. Based on field relationships, this metamorphism predated, and thus was unrelated to, the emplacement of granitoid plutons (for example, Esmailabad Granite) into the complex.

Chamgoo and Anarg Granodiorites.—The Chamgoo Mountain in the northernmost part of the Saghand area exposes a composite igneous intrusion that ranges in composition from quartz-monzodiorite to granite and intrudes the greenstones and marbles of the Poshteh-Badam Complex. Because of the apparent lithologic similarities of the Chamgoo intrusion to the Ariz and Polo-Mountain Granodiorites (Eastern Domain), Haghipour and Pelissier (1977) placed this pluton in their Precambrian "d" intrusive unit. Mafic enclaves particularly rich in biotite are common throughout the intrusion.

A composite granite-granodiorite intrusion somewhat similar in lithology to the Chamgoo Granodiorite crops out further south in the vicinity of the abandoned Anarg lead-zinc mine (fig. 3). This intrusion (informally named Anarg Granodiorite) was placed by Haghipour and Pelissier (1977) in their "gd" intrusive unit of presumed Precambrian age, along with the Daranjir Diorite of the Western Lithotectonic Domain.

Esmailabad Granite.—The metamorphic rocks of the Poshteh-Badam Complex were intruded by numerous bodies of a generally coarse-grained, pink-colored, granite known as the Esmailabad Granite (Haghipour and Pelissier, 1977). The largest contiguous outcrop of this intrusion occurs to the south of the Esmailabad village (fig. 3), where it has been the subject of systematic sampling for this study.

In the Rahneshk Mountain area, the Esmailabad Granite intrudes massive, fusulinid-bearing limestones of Permian age and is in turn overlain by the Cretaceous conglomerates and sandstones. Haghipour and Pelissier (1977) placed this pluton in a separate class, namely the "g3" intrusive unit of post-Permian and pre-Cretaceous age.

Western Lithotectonic Domain

The Western Lithotectonic Domain occupies the area to the west of the east-dipping Neybaz-Chatak (thrust) Fault. It terminates sharply to the west against the NE-trending Chapedony Fault. The Western Domain is dominated by the high-grade metamorphic rocks of the Chapedony Complex that are exposed along a number of flat-top, low-relief, topographic features known as "kalut" in the local dialect (for example, Kalut-e-Chatak). Apart from the migmatites and anatectic granites associated with its high-grade rocks, the Chapedony Complex is intruded by two large plutons in the southern part of the domain. These are the Daranjir Diorite and Khoshoumi Granite, named informally after the mountainous areas in which they crop out.

Chapedony Complex.—The assemblage of rocks that constitutes the Chapedony Complex (Hushmandzadeh, ms, 1969; Haghipour and Pelissier, 1977) is predominated by a variety of high-grade gneisses and associated migmatites. These rocks which represent the highest grade of metamorphism in the region were viewed as the oldest outcrops of Precambrian basement in central Iran (Haghipour, ms, 1974; Stöcklin, 1974). The complex is invariably in fault contact with the lower-grade or unmetamorphosed rocks in its immediate vicinity.

The dominant mineral assemblage of the Chapedony gneisses (K-feldspar, plagioclase and biotite) is inconclusive of any specific metamorphic grade. Nevertheless, coexistence with migmatites and anatectic granites implies metamorphism at or near the upper amphibolite facies conditions. An important compositional feature of the Chapedony gneisses is the complete absence of metamorphic aluminosilicate minerals (for example, sillimanite and andalusite) from these rocks which is probably due to the Al-poor (magmatic?) affinity of its precursors.

Daranjir Diorite.—A single pluton of mainly intermediate (dioritic) composition is exposed in the Daranjir Mountain, in the southern portion of the Western Domain. This intrusion, together with the Anarg Granodiorite (Central Domain) was assigned a Precambrian age (g1 or gd) by Haghipour and Pelissier (1977). The Daranjir Diorite is intruded by the Khoshoumi Granite along its eastern perimeters. This occurrence forms the only exposed contact of the diorite.

Khoshoumi Granite.—This large granitic pluton is exposed to the west of the Khoshoumi Mountain adjacent to the Daranjir Diorite. It was assigned by Haghipour and Pelissier (1977) a post-Permian and pre-Cretaceous age (g3), based on its lithologic similarities to the Esmailabad Granite (Central Domain). The Khoshoumi Granite intrudes both the Chapedony Complex and the Daranjir Diorite. Its probable offshoots in the form of pink, aplitic dikes are widespread throughout the Khoshoumi-Daranjir area.

U-Pb Geochronology

Samples of plutonic, metamorphic, volcanic and volcaniclastic rocks were collected from the main lithostratigraphic units of the Saghand region, incorporating all three of its lithotectonic domains. Table 1 lists 95 isotopic analyses that were performed on 22 rock specimens collected from 13 different rock units. All of the reported ages are based on U and Pb isotopic measurements on single- or multi-grain fractions of hand-selected zircon. Sample preparation and analytical techniques used in this study are described in detail by Ramezani (ms, 1997) and are largely similar to those of Krogh (1973; 1982a, b). All measurements were made at Washington

TABLE 1

U-Pb data from rock units of the Saghand area, central Iran

Fractions		Concentrations [2]					Atomic Ratios [4]					Age (Ma)
Analysis no.	Properties [1]	Wt. (μg)	U (ppm)	Pb_{rad} (ppm)	Pb_{common} (pg)	Th/U [3]	$^{206}Pb/^{204}Pb$	$^{206}Pb/^{238}U$ ±		$^{207}Pb/^{235}U$ ±		$^{207}Pb/^{206}Pb$ ±	$^{207}Pb/^{206}Pb$
Boneh-Shurow Complex													
A- Granitic gneiss from Gelmandeh Mountain (JR94-G8)													
1	FF, 12 equant prisms	8	359.2	30.65	5.9	0.519	2382	0.08096	11	0.6483	12	0.05808 08	532.7
2	FF, 10 equant prisms	5	299.4	25.14	11.9	0.562	605	0.07876	10	0.6273	20	0.05777 17	520.9
3	FF, 10 equant prisms	6	345.6	27.64	31.1	0.471	327	0.07679	13	0.6134	24	0.05793 21	527.1
4	FF, 29 needles	8	387.3	24.86	10.4	0.438	1256	0.06194	07	0.4863	09	0.05695 09	489.5
5	FF, 7 needles	2	220.2	14.20	6.8	0.444	292	0.06201	11	0.4909	47	0.05741 53	507.4
6	FF, 10 needles	3	347.1	22.30	15.7	0.457	249	0.06184	11	0.4797	37	0.05626 41	462.5
B- Granitic gneiss from Zamanabad Mountain (JR95-G42)													
1	MI, 3 equant prisms	2	776.1	65.04	2.5	0.416	3159	0.08174	16	0.6552	19	0.05814 14	534.9
2	MI, 1 single equant	1	1068	94.62	2.3	0.528	3031	0.08388	18	0.6730	22	0.05819 15	536.8
3	MI, 2 equant prisms	2	579.8	50.75	2.1	0.447	2772	0.08466	16	0.6819	23	0.05841 18	545.3
C- Granitic gneiss from Poshteh-Sorkh Mountain (JR94-G7)													
1	MI, 9 needles	3	252.1	22.26	8.1	0.416	556	0.08610	14	0.6923	31	0.05832 24	541.6
2*	MI, 7 equant prisms	2	257.0	22.46	13.4	0.356	255	0.08666	19	0.6997	60	0.05856 48	550.8
3*	MI, 6 equant prisms	12	272.4	26.50	4.6	0.194	4359	0.09583	13	0.9639	17	0.07295 07	1012.6
4*	MI, 8 equant prisms	7	138.2	23.61	16.9	0.301	569	0.15837	89	2.1064	134	0.09646 28	1556.8
5*	MI, 1 large prism	4	194.8	49.82	7.2	0.481	1560	0.23468	28	3.5891	55	0.11092 12	1814.6
D- Garnet-amphibolite from Boneh-Shurow Mountain (JR94-G11)													
1	MI, 1 very large prism	38	344.4	31.26	2.1	0.430	34413	0.08822	12	0.7116	10	0.05850 03	548.7
2	MI, 5 large prisms	17	444.7	40.24	2.1	0.421	21109	0.08813	11	0.7101	09	0.05843 04	546.1
3	FF, 20 small equant	10	137.9	11.72	4.7	0.331	1670	0.08488	16	0.6805	18	0.05815 14	535.3
4	FF, 6 small equant	6	58.5	4.65	2.3	0.299	744	0.08002	15	0.6438	62	0.05835 54	543.1

TABLE 1
(continued)

Fractions		Concentrations [2]					Atomic Ratios [4]					Age (Ma)
Analysis no.	Properties [1]	Wt. (μg)	U (ppm)	Pb_{rad} (ppm)	Pb_{common} (pg)	Th/U [3]	$^{206}Pb/^{204}Pb$	$^{206}Pb/^{238}U$ ±		$^{207}Pb/^{235}U$ ±		$^{207}Pb/^{206}Pb$ ±	$^{207}Pb/^{206}Pb$
Boneh-Shurow Complex													
E- Quartz-diorite from Boneh-Shurow Mountain (JR94-G12)													
1	MI, 3 flat prisms	4	926.6	89.66	1.7	0.668	11888	0.08830	10	0.7120	09	0.05848 05	547.8
2	MI, 4 equant prisms	5	718.6	67.22	5.2	0.538	4307	0.08829	09	0.7117	09	0.05847 05	547.3
3	MI, 1 long prism	3	213.2	20.08	2.1	0.582	1657	0.08790	13	0.7097	34	0.05856 26	550.8
F- Mica-schist from Eskambilo Mountain (JR95-G31)													
1	MI, 4 equant prisms	3	378.9	40.29	2.5	0.548	2889	0.10002	16	0.8322	23	0.06034 16	614.5
2	MI, 1 equant prism	2	295.4	30.82	2.4	0.470	1588	0.10047	15	0.8318	38	0.06004 26	617.2
3	MI, 1 equant prism	2	156.4	19.47	1.5	1.303	1301	0.09783	23	0.8090	60	0.05997 41	601.7
Tashk Formation													
G- Tuffaceous rock from Tashk Mountain (JR95-G40)													
1	MI, 1 prism	2	261.7	35.22	1.9	1.480	1450	0.10203	18	0.8520	49	0.06056 33	623.7
2	MI, 1 long prism	1	347.9	35.13	3.9	0.306	547	0.10134	55	0.8512	86	0.06092 53	636.5
3	MI, 1 prism	1	81.8	10.89	1.5	0.829	354	0.11654	42	1.0204	225	0.06351 133	725.3
4	MI, 1 round grain	2	36.5	5.24	1.6	0.690	449	0.13049	39	1.1669	202	0.06485 107	769.6
5	MI, 1 prism	1	96.0	14.53	1.6	0.934	511	0.13013	36	1.1622	168	0.06478 89	767.1
6	MI, 1 equant prism	2	111.2	16.06	2.2	0.529	818	0.13657	21	1.2425	97	0.06598 49	805.8
7	MI, 1 red prism	1	864.0	279.14	2.6	0.130	8563	0.32592	39	5.1220	67	0.11398 08	1863.8
8	MI, 1 red round grain	1	450.0	157.44	1.7	0.395	7202	0.33012	45	5.2086	72	0.11443 10	1870.9
Cambrian Volcano-Sedimentary Unit (CVSU)													
H- Rhyodacite from Douzakh-Darreh Mountain (JR94-G28)													
1	MI, 11 needles	7	239.4	22.63	2.1	0.759	4282	0.08547	11	0.6843	15	0.05807 11	532.5
2	MI, 12 prisms	25	233.8	21.58	1.9	0.617	17007	0.08535	14	0.6825	11	0.05800 05	529.8
3	MI, 20 short prisms	19	278.1	25.80	1.8	0.643	16182	0.08525	11	0.6815	09	0.05797 04	528.8

TABLE 1
(continued)

Fractions		Concentrations [2]					Atomic Ratios [4]						Age (Ma)
Analysis no.	Properties [1]	Wt. (μg)	U (ppm)	Pb_{rad} (ppm)	Pb_{common} (pg)	Th/U [3]	$^{206}Pb/^{204}Pb$	$^{206}Pb/^{238}U$	±	$^{207}Pb/^{235}U$	±	$^{207}Pb/^{206}Pb$ ±	$^{207}Pb/^{206}Pb$
Cambrian Volcano-Sedimentary Unit (CVSU)													
H- Rhyodacite from Douzakh-Darreh Mountain (JR94-G28)													
4	MI, 1 large prism	8	264.4	23.85	1.6	0.528	7645	0.08543	10	0.6837	11	0.05804 07	531.4
I- Dacite-porphyry from Zarigan Mountain (JR95-47)													
1	MI, 11 equant grains	21	33.2	3.06	2.4	0.610	1656	0.08530	10	0.6823	28	0.05801 22	530.2
2	MI, 3 equant grains	4	35.7	3.28	1.7	0.591	539	0.08547	22	0.6904	113	0.05858 91	551.6
3	MI, 1 equant grain	2	37.1	3.43	1.6	0.627	326	0.08534	27	0.6901	190	0.05865 155	554.0
Cambrian Granite-Tonalite Intrusions													
J- Granodiorite from Ariz Mountain (JR95-G54)													
1	FF, 4 equant prisms	7	315.0	28.65	4.9	0.551	2558	0.08558	11	0.6849	13	0.05804 09	531.3
2	FF, 1 equant prism	4	327.0	29.93	1.8	0.570	4221	0.08574	18	0.6875	22	0.05816 15	535.8
3	FF, 1 prism	4	272.1	26.10	1.9	0.763	2781	0.08554	11	0.6857	22	0.05814 16	535.0
4	FF, 3 small prisms	2	156.4	14.64	1.5	0.687	1105	0.08508	16	0.6830	55	0.05822 44	538.1
K- Granodiorite from Polo Mountain (JR94-G14)													
1	FF, 5 prisms	3	288.8	26.37	1.8	0.585	2944	0.08512	19	0.6804	23	0.05797 15	528.8
2	FF, 3 small prisms	3	173.6	15.95	1.4	0.615	2069	0.08503	22	0.6808	35	0.05807 29	532.2
3	FF, 19 needles	9	377.0	33.84	2.9	0.582	6435	0.08384	10	0.6689	09	0.05787 06	524.9
4	FF, 16 needles	7	372.8	34.02	11.1	0.686	1371	0.08293	13	0.6590	12	0.05763 10	515.7
5	FF, 11 needles	8	401.5	35.55	16.3	0.649	1102	0.08129	09	0.6467	11	0.05770 08	518.3
6*	FF, 12 equant prisms	8	198.9	19.16	7.9	0.639	1188	0.08857	13	0.7200	17	0.05896 11	565.7
7*	FF, 14 equant prisms	9	241.8	24.29	9.3	0.501	1407	0.09422	41	0.8566	55	0.06594 33	804.6
Cambrian Trondhjemite Intrusions													
L- Zarigan Leucogranite from Poshteh-Sorkh Mountain (JR94-G1)													
1	FF, 5 prisms	12	240.0	21.75	2.9	0.522	5344	0.08592	10	0.6895	12	0.05820 08	537.3

TABLE 1
(continued)

Fractions		Concentrations [2]					Atomic Ratios [4]						Age (Ma)
Analysis no.	Properties [1]	Wt. (μg)	U (ppm)	Pb_{rad} (ppm)	Pb_{common} (pg)	Th/U [3]	$^{206}Pb/^{204}Pb$	$^{206}Pb/^{238}U$	±	$^{207}Pb/^{235}U$	±	$^{207}Pb/^{206}Pb$ ±	$^{207}Pb/^{206}Pb$
Cambrian Trondhjemite Intrusions													
L- Zarigan Leucogranite from Poshteh-Sorkh Mountain (JR94-G1)													
2	FF, 2 prisms	5	203.9	18.02	5.1	0.427	983	0.08597	09	0.6890	29	0.05813 23	534.6
3	FF, 5 needles	5	227.3	20.50	13.1	0.505	486	0.08595	11	0.6893	37	0.05816 29	535.8
4	FF, 6 equant prisms	12	265.4	23.59	3.5	0.431	4775	0.08634	13	0.6964	13	0.05850 08	548.5
5	FF, 6 equant prisms	12	219.2	19.53	2.9	0.432	4768	0.08654	15	0.6965	15	0.05837 09	543.7
M- Zarigan Leucogranite from Zarigan Mountain (JR94-G3)													
1	FF, 5 prisms	15	218.1	19.87	5.4	0.552	3460	0.08574	11	0.6868	10	0.05809 06	533.3
2	FF, 7 equant prisms	11	264.1	24.27	4.4	0.560	3600	0.08632	09	0.6942	11	0.05833 07	542.2
3	FF, 13 needles	8	227.9	21.00	4.4	0.545	2426	0.08682	09	0.6970	14	0.05823 10	538.3
4	FF, 1 large prism	6	210.8	23.55	6.2	0.817	1218	0.09819	18	0.8235	23	0.06083 14	633.1
5	FF, 20 equant prisms	23	265.0	24.91	3.2	0.551	11070	0.08828	10	0.7276	09	0.05977 04	595.4
6*	FF, 1 large prism	10	185.5	33.95	2.7	0.233	7316	0.17233	17	2.5548	28	0.10752 06	1757.8
N- Leucogranite from Douzakh-Darreh Mountain (JR95-G38)													
1	MI, 2 prisms	2	215.2	20.51	1.5	0.763	1926	0.08499	15	0.6787	31	0.05792 25	526.7
2	MI, 1 prism	3	183.0	17.35	1.7	0.739	1598	0.08509	20	0.6807	40	0.05802 31	530.7
3	MI, 8 small prisms	4	235.1	22.27	1.4	0.740	3850	0.08496	14	0.6811	18	0.05815 13	535.3
4	MI, 1 prism	2	171.3	15.73	2.3	0.627	700	0.08476	21	0.6780	69	0.05801 57	530.2
O- Sefid Granite (JR94-G13)													
	MI, 36 turbid prisms	6	4968.3	375.52	54.9	0.260	2676	0.07698	09	0.6144	07	0.05789 03	525.7
Triassic Granite-Tonalite Intrusion													
P- Granite from Chamgoo Mountain (JR95-G50)													
1	MI, 1 prism	2	975.4	32.96	2.1	0.365	1852	0.03367	05	0.2335	12	0.05031 24	209.4
2	MI, 4 prisms	3	532.5	18.42	2.0	0.436	1604	0.03371	05	0.2353	14	0.05062 28	223.5

TABLE 1
(continued)

Fractions			Concentrations [2]				Atomic Ratios [4]						Age (Ma)
Analysis no.	Properties [1]	Wt. (μg)	U (ppm)	Pb_{rad} (ppm)	Pb_{common} (pg)	Th/U [3]	$^{206}Pb/^{204}Pb$	$^{206}Pb/^{238}U$	±	$^{207}Pb/^{235}U$	±	$^{207}Pb/^{206}Pb$ ±	$^{207}Pb/^{206}Pb$
Triassic Granite-Tonalite Intrusion													
P- Granite from Chamgoo Mountain (JR95-G50)													
3	MI, 1 prism	3	433.5	14.83	1.5	0.391	1717	0.03373	09	0.2362	17	0.05080 34	231.5
4	MI, 2 small prisms	1	798.2	27.02	1.5	0.411	1359	0.03363	05	0.2315	18	0.04993 36	191.6
Q- Esmailabad Granite (JR94-G16)													
1	FF, 2 large prisms	8	920.3	31.13	1.9	0.311	8470	0.03415	04	0.2377	04	0.05049 06	217.6
2	FF, 1 large zircon	8	552.4	18.80	8.2	0.326	1138	0.03421	05	0.2381	06	0.05047 12	216.8
3	FF, 17 needles	8	925.4	31.19	1.7	0.326	9631	0.03387	04	0.2360	04	0.05054 05	219.8
4	FF, 50 needles	21	1029.4	34.48	6.2	0.329	7424	0.03361	04	0.2356	03	0.05084 03	233.4
5	FF, 5 large prisms	10	1026.1	32.11	5.9	0.284	3478	0.03181	04	0.2220	03	0.05062 05	223.6
6	FF, 14 prisms	12	1023.5	34.75	2.7	0.280	10275	0.03443	04	0.2454	03	0.05170 04	272.3
Chapedony Complex													
R- Porphyroblastic gneiss from Kalut-e-Chapedony (JR94-G18)													
1	FF, 10 prisms	14	1034.9	7.80	7.2	0.449	977	0.00733	01	0.0475	02	0.04698 14	48.2
2	FF, 20 needles	11	1223.1	8.94	5.5	0.415	1149	0.00716	02	0.0465	02	0.04710 16	54.2
3	FF, 1 large prism	13	1230.6	8.37	3.6	0.197	2069	0.00710	01	0.0461	02	0.04713 15	55.6
S- Biotite-gneiss from Neybaz Mountain (JR94-G23)													
1	MI, 1 prism	6	929.7	6.75	1.2	0.331	2084	0.00730	01	0.0473	02	0.04701 21	49.7
2	MI, 30 small needles	10	1935.2	14.05	2.4	0.306	3917	0.00732	01	0.0477	01	0.04722 10	60.1
3	MI, 12 equant prisms	6	1529.3	11.33	1.8	0.281	2568	0.00753	01	0.0490	02	0.04723 18	61.0
4	MI, 3 prisms	16	1036.1	7.68	2.9	0.171	2878	0.00774	01	0.0508	01	0.04760 11	79.4
5*	MI, 6 trapezohedra	14	1036.4	9.04	2.3	0.032	3746	0.00906	01	0.0673	01	0.05386 11	365.3
T- Migmatitic leucosome from Neybaz Mountain (JR94-G21)													
1	MI, 3 prisms	6	569.7	4.41	5.3	0.341	315	0.00773	05	0.0504	08	0.04727 68	62.8

TABLE 1
(continued)

Analysis no.	Fractions Properties [1]	Wt. (μg)	Concentrations [2] U (ppm)	Pb_{rad} (ppm)	Pb_{common} (pg)	Th/U [3]	Atomic Ratios [4] $^{206}Pb/^{204}Pb$	$^{206}Pb/^{238}U$ ±	$^{207}Pb/^{235}U$ ±	$^{207}Pb/^{206}Pb$ ±	Age (Ma) $^{207}Pb/^{206}Pb$
Chapedony Complex											
T- Migmatitic leucosome from Neybaz Mountain (JR94-G21)											
2	MI, 20 needles	7	2098.1	15.53	5.3	0.114	1373	0.00769 03	0.0508 02	0.04792 19	95.2
3	MI, 4 prisms	7	2077.3	22.72	4.0	0.043	2805	0.01146 02	0.0826 02	0.05230 09	298.6
4*	MI, 5 trapezohedra	6	916.8	44.40	16.6	0.046	920	0.04503 18	0.8271 34	0.13322 15	2140.9
Eocene Diorite/Granite Intrusions											
U- Diorite from Daranjir Mountain (JR95-G30)											
1	FF, 2 large equant	13	864.7	7.47	2.7	1.256	1778	0.00676 01	0.0439 02	0.04714 20	56.5
2	FF, 2 large prisms	12	534.9	4.75	2.0	1.333	1506	0.00679 04	0.0442 04	0.04719 35	59.0
3	FF, 2 flat prisms	9	655.4	5.71	3.3	1.263	817	0.00676 02	0.0440 03	0.04720 36	59.3
V- Granite from Khoshoumi Mountain (JR94-G27)											
1	FF, 18 small needles	11	822.9	5.77	1.5	0.408	2707	0.00691 01	0.0447 02	0.04690 17	44.2
2	FF, 6 prisms	8	778.3	5.4	1.5	0.377	1831	0.00689 02	0.0446 03	0.04695 27	46.7
3	FF, 1 very large prism	23	1672.5	11.34	1.7	0.197	9965	0.00709 01	0.0460 01	0.04701 07	49.8
4	FF, 8 equant prisms	25	717.0	7.32	2.0	0.106	5844	0.01009 01	0.0707 01	0.05086 08	234.4

NOTES: [1] Zircon fractions were selected from non-paramagnetic mineral separates in the final Frantz (FF) magnetic separation, or from heavy-mineral precipitates in methylene iodide (MI).
[2] Uncertainty in weight is 0.0002 mg (2σ). Concentrations of U and Pb_{rad} are known to better than 10%.
[3] Calculated Th/U ratio assuming that all ^{208}Pb in excess of blank, common Pb and spike is radiogenic.
[4] Corrected for fractionation, spike, laboratory blank and initial common Pb. Absolute uncertainties are reported as 2σ after the ratios and refer to the final digits.
Mass fractionation correction of 0.09% and 0.11% per atomic mass unit for Pb and U, respectively.
Total laboratory blank averaged 2 pg for Pb and less than 0.2 pg for U.
Age calculations based on the decay constants of Jaffey and others (1971).
Initial common Pb compositions from the Pb evolution model of Stacey and Kramers (1975) at the interpreted age of the rock.
H Analysis with strong zircon inheritance, plotting outside the field of view on concordia diagrams.

University on a VG Sector-54 solid-source mass spectrometer equipped with a Daly photomultiplier and in an ion-counting mode.

The measured isotopic ratios, U and Pb concentrations, calculated atomic ratios and ages are given in table 1. Age uncertainties were calculated using an error propagation algorithm similar to Ludwig (1980) and were plotted as ellipses on conventional U-Pb concordia diagrams (figs. 4 to 8). Age and associated uncertainties are estimated by one of two means; for the majority of the concordant analyses, the sample age was calculated from the weighted average $^{207}Pb/^{206}Pb$ age of its individual zircon analyses. In a few cases, however, the weighted average $^{206}Pb/^{238}U$ age was considered the best age estimate because of its low sensitivity to common Pb correction. For discordant analyses with variable $^{207}Pb/^{206}Pb$ ages, regression calculations were applied, where feasible, using the ISOPLOT algorithm of Ludwig (1991). All ages are reported at 95 percent confidence limits.

Neoproterozoic Rocks

The Neoproterozoic Era represents the time period between the end of Mesoproterozoic (approximately 900 Ma) and the start of Cambrian. The 545 Ma age is herein recognized as the Neoproterozoic-Cambrian boundary, following the recent time-scale calibrations of Bowring and others (1993) and Tucker and McKerrow (1995). Similarly, termination of the Early Cambrian Epoch and the Cambrian-Ordovician boundary are placed at 518 Ma and 495 Ma, respectively (Tucker and McKerrow, 1995). The Geological Society of America geologic time scale (1999) is used for the remainder of the Phanerozoic Eon.

The Neoproterozoic rocks of the Saghand region are exclusive to the Eastern Domain and have not been observed in any of the other lithotectonic domains. These rocks are characteristic of the Kashmar-Kerman Tectonic Zone among the constituent elements of the Central Iranian Terrane.

Boneh-Shurow Complex.—Three samples of quartzofeldspathic gneiss from the Boneh-Shurow Complex collected from the Poshteh-Sorkh Mountain, Kalut-e-Gelmandeh and the Zamanabad Mountain (fig. 3) were analyzed for age determination. Ten fractions of prismatic zircon, including a single-grain, from these samples show variable degrees of age discordance (1.8% to 16.9%) because of variable amounts of post-crystallization lead-loss. All ten analyses tend to plot along a well-defined discordia line on the concordia plot (fig. 4A), with a regressed upper intercept age of 544 ± 7 Ma. This age is consistent with the concordia intercept ages of zircon from each individual gneiss sample and is interpreted as the crystallization age of the granitic protolith(s) of the Boneh-Shurow gneiss.

A sample of garnet-amphibolite from the Boneh-Shurow Complex contained two morphologically distinct varieties of zircon: small, round, clear grains and a distinct population of large (0.2 mm in diameter), amber-colored, blocky zircon. Based on the zircon morphology, mafic composition of the rock and its metamorphic grade, both zircon varieties are most likely to be of metamorphic origin. Two analyses of the amber zircon, including a single-grain analysis, produced concordant ages with a weighted average $^{207}Pb/^{206}Pb$ age of 547.6 ± 2 Ma (fig. 4B), whereas the clear zircon fractions were significantly discordant (up to 9%). The latter age serves as the best estimate for the timing of peak-metamorphism of the Boneh-Shurow garnet-amphibolite.

Two multi-grain and one single-grain zircon fractions from a Boneh-Shurow quartz-diorite intrusion yielded concordant analyses with an average $^{207}Pb/^{206}Pb$ age of 547.6 ± 2.5 Ma (fig. 4C). This age reflects the timing of post-metamorphic quartz-diorite emplacement into the complex. The notable similarity between the latter age and that of the metamorphic zircon in the host garnet-amphibolite implies that late-stage magmatic intrusion must have occurred shortly (within a maximum of 4.5 Ma) after the peak-metamorphism near the Precambrian-Cambrian boundary.

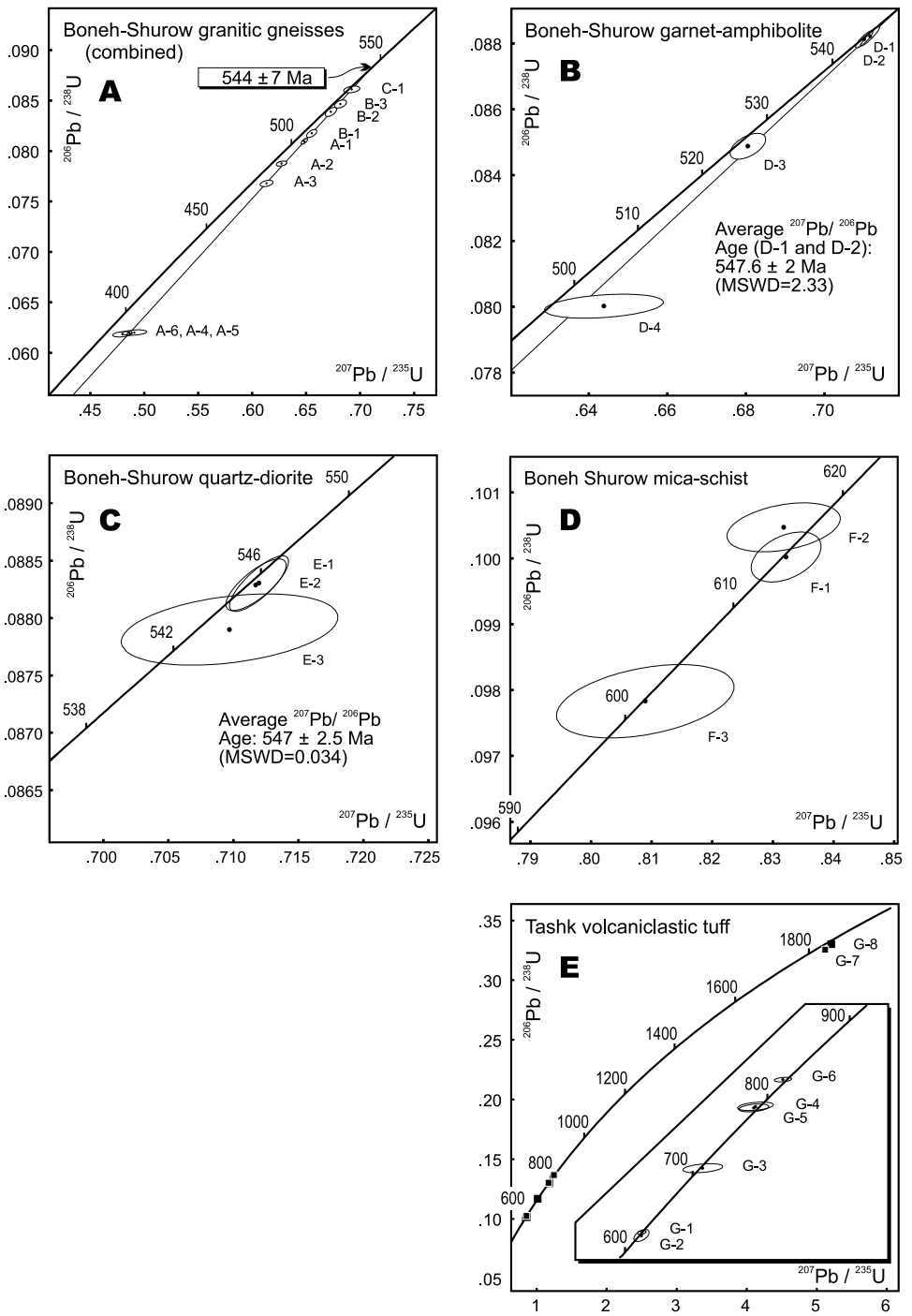

Fig. 4. Concordia diagrams for the late Neoproterozoic rocks of the Saghand area.

Three zircon fractions, including 2 single grains analyzed from a sample of Boneh-Shurow mica-schist produced concordant ages (fig. 4D), ranging from 602 Ma to 617 Ma ($^{207}Pb/^{206}Pb$ ages). Considering the low metamorphic grade of this rock and its pelitic composition, all of the analyzed zircons are likely to be of detrital origin.

Tashk Formation.—Separated zircon from a sample of volcaniclastic tuff from this formation defines two general morphologic groups: clear, colorless prisms, and orange-brown, variably round grains. Six single-grain analyses of clear zircon are all concordant within error, but range in age from 623 Ma to 806 Ma (fig. 4E). The great majority of these grains are evidently of detrital (reworked igneous) origin. The two youngest analyses overlap within error, with a weighted average $^{207}Pb/^{206}Pb$ age of 627 ± 19 Ma. This age provides an upper limit for the timing of deposition of the Tashk Formation, as the presence of yet younger, but unidentified, zircon in the rock cannot be ruled out.

Single grains of orange-brown zircon from the same sample yielded discordant ages that are significantly older ($^{207}Pb/^{206}Pb$ ages of 1864 Ma and 1871 Ma) than those of the colorless variety. These detrital grains apparently originated from a different source rock of possibly Early Proterozoic age.

Our data delimit the overall deposition age of the Tashk Formation between 627 Ma and 533 Ma, the latter being the intrusion age of the oldest granitic plutons (for example, Ariz Granodiorite) emplaced into the formation. A general late Neoproterozoic to Early Cambrian age is thus assigned to the Tashk Formation as a whole.

Early Cambrian Rocks

The Early Cambrian rocks are predominant in the Eastern Domain, with some limited occurrences in the Central Domain. The most notable of this group are the Cambrian Volcano-Sedimentary Unit, Ariz and Polo-Mountain granodiorites, Zarigan Leucogranite and the Douzakh-Darreh Leucogranite. The chronostratigraphic equivalents of the Early Cambrian rocks are exposed throughout the Kashmar-Kerman Tectonic Zone, both to the north and south of the Saghand region (fig. 2).

Cambrian Volcano-Sedimentary Unit.—Analyzed rocks from this unit include a volcanic rhyodacite from the Douzakh-Darreh Mountain and a sub-extrusive dacite-porphyry from the Zarigan Mountain. The eruption age of the rhyodacite is constrained at 528.2 ± 0.8 Ma (average $^{206}Pb/^{238}U$ age) by the concordant analyses of four prismatic zircon fractions (fig. 5A).

Zircon from the dacite-porphyry is generally subhedral and spindle-shaped, with exceptionally low U and radiogenic Pb contents (less than 40 ppm and 4 ppm, respectively). Despite relatively large analytical uncertainties in their calculated $^{207}Pb/^{235}U$ and $^{207}Pb/^{206}Pb$ ages, all three analyses from this rock are concordant within error and overlap in age (fig. 5B). Their weighted average $^{206}Pb/^{238}U$ age of 527.9 ± 1 Ma thus provides a reliable estimate for the timing of dacite-porphyry emplacement.

The measured ages provide conclusive evidence that the CVSU (formerly known as Infracambrian) was deposited well into the Early Cambrian Epoch and it is not Precambrian in age.

Granite-Tonalite Intrusions.—The composite igneous intrusions of granite to tonalite composition throughout the Eastern Domain are best represented by the Ariz Granodiorite in the south. Analyses of two single-grain and two multi-grain zircon fractions from a sample of granodiorite are all concordant and overlap in age (fig. 5C). Their average $^{207}Pb/^{206}Pb$ age of 533 ± 1 Ma best represents the age of emplacement of the pluton. This age is consistent with the less precise zircon age (upper concordia intercept) of 530 ± 21 Ma measured from the Polo-Mountain Granodiorite (fig. 5C) at the northernmost exposures of the Eastern Domain.

The great majority of the Early Cambrian granite-tonalite intrusions were emplaced into the terrigenous and volcaniclastic strata of the Tashk Formation. Their

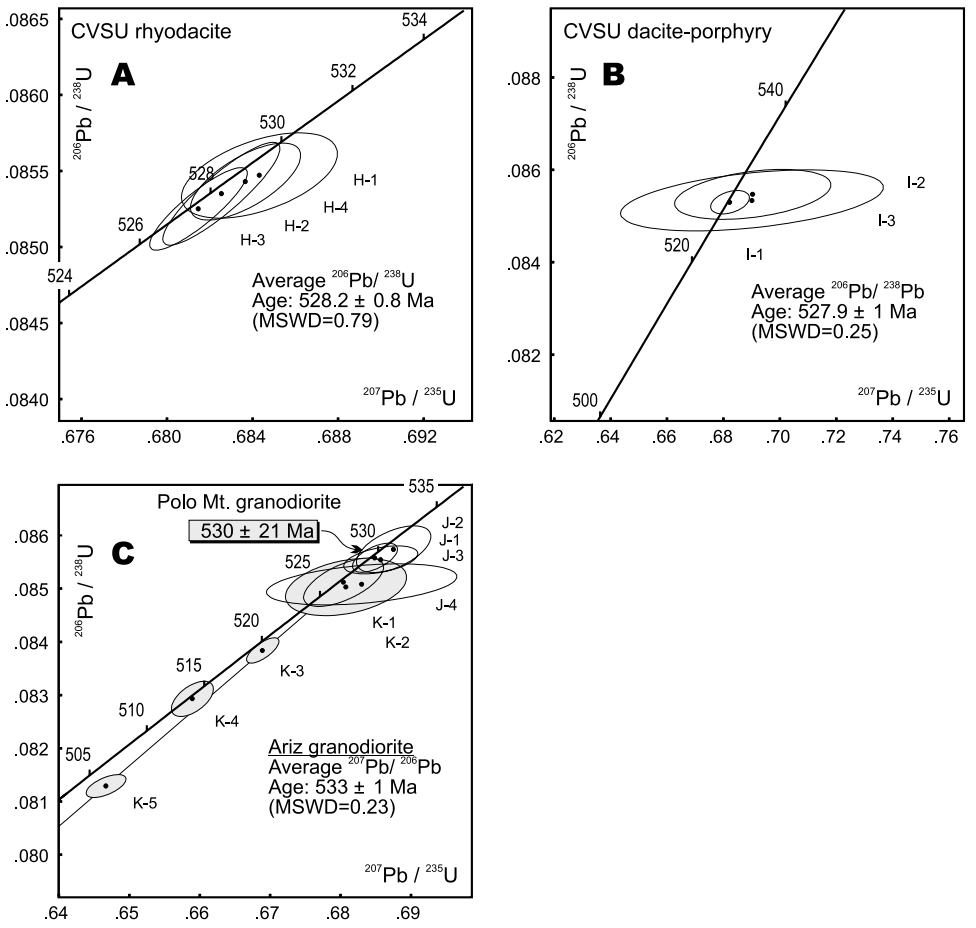

Fig. 5. Concordia diagrams for the Early Cambrian volcanic and granitic rocks of the Saghand area.

crystallization age, therefore, places a reliable lower limit on the deposition age of the Tashk Formation.

Leucogranite (trondhjemite) Intrusions.—Shallow-intrusive, felsic rocks of the Zarigan Leucogranite and its associated intrusive bodies (for example, Douzakh-Darreh leucogranite and Sefid Granite) constitute the largest volume of igneous rocks throughout the Saghand region. The emplacement of these plutons marks a pivotal episode in the thermotectonic evolution of the Eastern Domain.

The crystallization age of the Zarigan intrusion is constrained by zircon analyses of two trondhjemite samples from its Poshteh-Sorkh (sample JR94-G1) and Zarigan (sample JR94-G3) outcrops (fig. 3). The analyses from both samples show evidence of inheritance from an older source(s), which are more conspicuous in the latter sample. Regression analysis of G1 data (5 analyses) yields concordia intercept ages of 529 ± 16 Ma and 1378 ± 858 Ma (fig. 6A). Similarly, four zircon analyses from G3 are regressed with high probability to a discordia line with calculated intercept at 525 ± 7 Ma and 784 ± 69 Ma (fig. 6B). Since most of the analyses plot at or near the lower concordia intercept, the lower intercept ages serve as good estimates for the emplacement age of the Zarigan leucogranite.

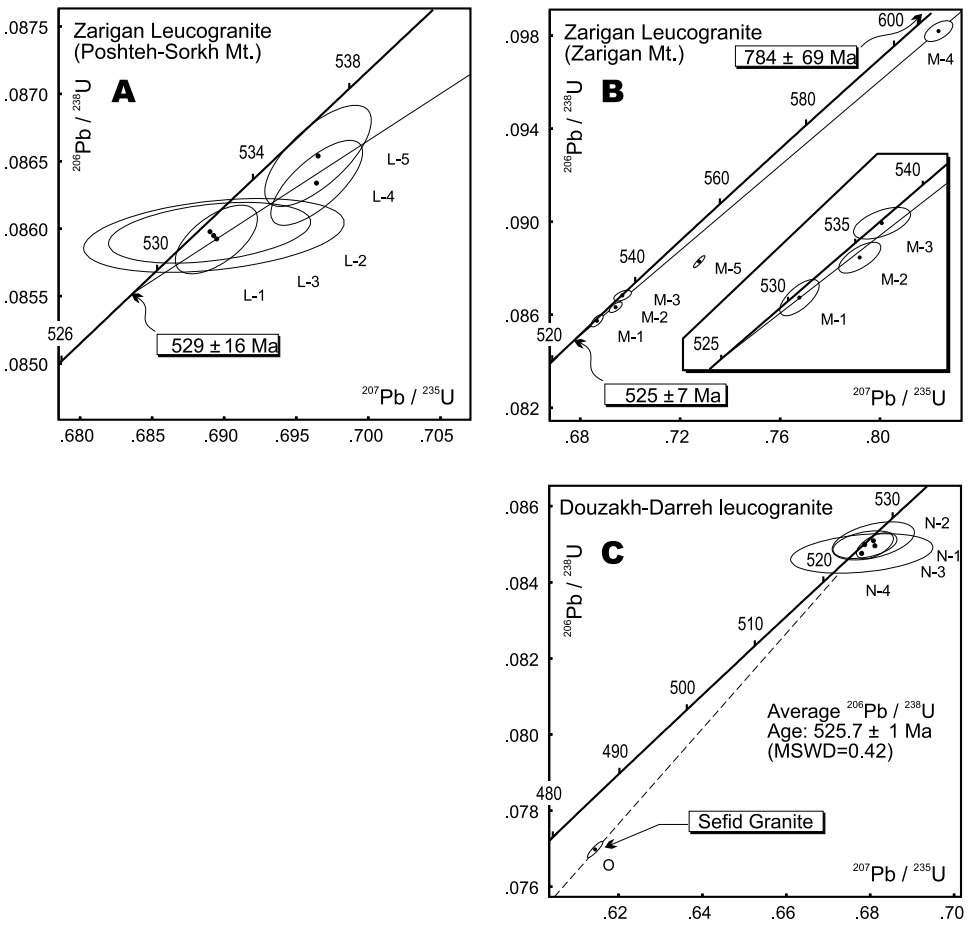

Fig. 6. Concordia diagrams for the Early Cambrian leucogranites of the Saghand area.

Four analyses of prismatic zircon, including two single-grain analyses, from a sample of the Douzakh-Darreh Leucogranite produced concordant and overlapping ages that show no evidence of lead-loss or zircon inheritance (fig. 6C). Therefore, their weighted average $^{206}Pb/^{238}U$ age of 525.7 ± 1 Ma with a fairly high probability is the best estimate for the emplacement age of the Douzakh-Darreh Leucogranite.

Separated zircon from the Sefid Granite were small and prismatic in shape, but highly turbid and of poor overall quality, probably because of extensive metamictization. The only zircon fraction analyzed from this sample (O) had unusually high concentrations of U (about 5000 ppm) and common Pb (total of 55 pg). Despite its high degree of discordance (9.4%), the $^{207}Pb/^{206}Pb$ age of this fraction (525.7 ± 2.4 Ma) coincides with zircon ages of other trondhjemite intrusions and can serve as an approximation for the emplacement age of the Sefid Granite (fig. 6C). This approximation is only plausible if Pb-loss in zircon was relatively recent.

Our new U-Pb zircon data clearly indicate that the Zarigan Leucogranite and its associated intrusions were emplaced in the mid-late Early Cambrian and do not belong to the Infracambrian, as previously speculated.

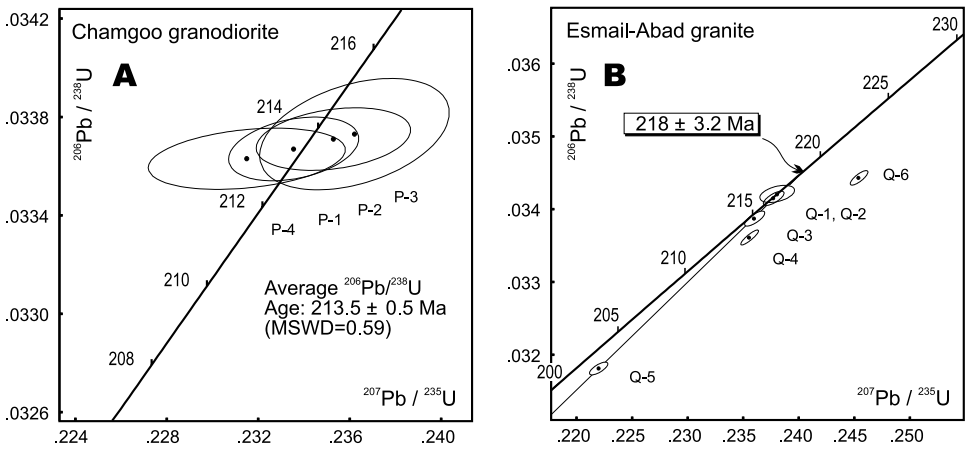

Fig. 7. Concordia diagrams for the Late Triassic rocks of the Saghand area.

Late Triassic Rocks

Plutonic rocks of Triassic age are represented by the Chamgoo and Anarg Granodiorites, as well as the Esmailabad Granite (fig. 3). These intrusions are exposed exclusively in the northern part of the Central Lithotectonic Domain and have not been identified elsewhere in the Saghand region. The age-equivalents of the Triassic plutons are generally unknown from the remainder of central Iran.

Granite-Tonalite Intrusions.—Four fractions of well-faceted, prismatic zircon (including two single grains) from a sample of the Chamgoo Granodiorite produced concordant analyses that overlap within analytical error, with a weighted average $^{207}Pb/^{206}Pb$ age of 215 ± 13 Ma (fig. 7A). The average $^{206}Pb/^{238}U$ age of all analyses is 213.5 ± 0.4 Ma, which is consistent with the former age.

The analyzed multi-grain zircon fractions from the Esmailabad Granite range from concordant (Q-1 and Q-2) to variably discordant (Q3 through Q-6, fig. 7B). Discordance appears to have been caused by a combination of lead-loss and inherited zircon from an older source. Nevertheless, four of the analyses regress with high probability to a discordia with calculated intercepts at 218 ± 3 Ma and −74 ± 93 Ma. The 218 ± 3 Ma approximates the emplacement age of the Esmailabad Granite.

Based on the measured U-Pb ages, the Chamgoo Granodiorite and the Esmailabad Granite (also Anarg Granodiorite, not reported here) were emplaced within a relatively short period of time in the Late Triassic. Their emplacement was evidently unrelated to the much older intrusion of granite-tonalite plutons (for example, Ariz) throughout the neighboring Eastern Domain, as previously depicted.

Eocene Rocks

The vigorously debated ages of the high-grade metamorphic and anatectic rocks of the Saghand region are now constrained by the new U-Pb data to be Tertiary (Middle Eocene). The occurrence of these rocks is entirely restricted to the Western Lithotectonic Domain. The Chapedony Complex, as well as the Khoshoumi and Daranjir intrusions, comprises the bulk of the Eocene rocks in the area.

Chapedony Complex.—Multiple samples of biotite-gneiss and migmatitic felsite from various outcrops of the Chapedony Complex were analyzed for age determination. Zircons from these samples display a variety of crystal habits including equant prisms and needles, as well as trapezohedral and tabular forms. The trapezohedral zircon, in

particular, produced conspicuously older and highly discordant ages due to the presence of old, inherited components.

Three prismatic zircon fractions (one single-grain and two multi-grain) from a porphyroblastic gneiss sample from the Kalut-e-Chapedony are concordant within analytical uncertainties (fig. 8A), but have different $^{206}Pb/^{238}U$ ages (47.1, 46.0 and 45.6 Ma). Zircon from this sample is consistently high in U(>1000 ppm) and appears to have experienced lead-loss at an even younger age. The weighted average $^{207}Pb/^{206}Pb$ age of all three fractions is 52.4 ± 9 Ma that represents a good estimate for the age of zircon crystallization in the rock.

A sample of biotite-gneiss from the Neybaz Mountain yielded a concordant (single-grain) and three variably discordant (multi-grain) zircon analyses (fig. 8B). The discordance is apparently due to variable amounts of inherited zircon from an older source(s). Three of the four analyses (S-1, S-3 and S-4, all prismatic zircons) define a discordia line with calculated intercepts at 46.8 ± 2.5 Ma and 502 ± 291 Ma. Similarly, the regression of three analyses of prismatic zircon from a sample of migmatitic felsite from the same locality resulted in a discordia with intercept ages at 46.3 ± 1.7 Ma and 616 ± 34 Ma (fig. 8C). The similarity in zircon age and inheritance patterns between the migmatitic felsite and its host biotite-gneiss is suggestive of coeval zircon crystallization in both rocks. The lower concordia intercept ages are thus best interpreted as the age of metamorphic/anatectic zircon crystallization in the Chapedony Complex. This interpretation is consistent with the observation that most of the analyses plot at or near the lower concordia intercept.

Based on the collective U-Pb age results from the high-grade gneisses and migmatites (including those not reported here), the main-stage or peak metamorphism of the Chapedony Complex must have occurred at approximately 46 Ma, in the Middle Eocene.

Diorite/Granite Intrusions.—A diorite sample from the Daranjir intrusion yielded well-faceted, prismatic zircon typical of those in plutonic rocks. Three double-grain zircon fractions produced concordant, overlapping analyses with average $^{207}Pb/^{206}Pb$ and $^{206}Pb/^{238}U$ ages of 57 ± 15 Ma and 43.4 ± 0.2 Ma, respectively (fig. 8D). Both ages agree within uncertainties and are interpreted as the emplacement age of the Daranjir intrusion.

Prismatic zircon by and large similar in habit to those in the Daranjir Diorite was recovered from a sample of the adjacent Khoshoumi Granite. Regression of four analyses, two of which were concordant, results in a discordia line with calculated intercepts at 44.3 ± 1.1 Ma and 544 ± 29 Ma (fig. 8E). The lower intercept age serves as the best estimate for the emplacement age of the Khoshoumi Granite.

The diorite and the granite overlap in age with one another and with the peak-metamorphism of the Chapedony Complex. Based on field relationships and isotopic ages, both plutons are defined as late- to post-metamorphic intrusions of Middle Eocene age.

GEOCHEMISTRY

A selected number of whole-rock samples from various igneous rocks of the Saghand region were analyzed for major and trace elements in order to, 1) compare their compositional characteristics both within and across the lithotectonic domain boundaries and, 2) draw inferences regarding their origin and possible tectonic environments. These are achieved in part by comparison with compositionally similar rocks of known geologic setting.

Analytical Methods

Whole-rock concentrations of major oxides, as well as the trace elements Ni, V, Pb, Zn, Sn, Rb, Sr, Ga, Nb, Zr and Y, were determined by the X-ray fluorescence (XRF)

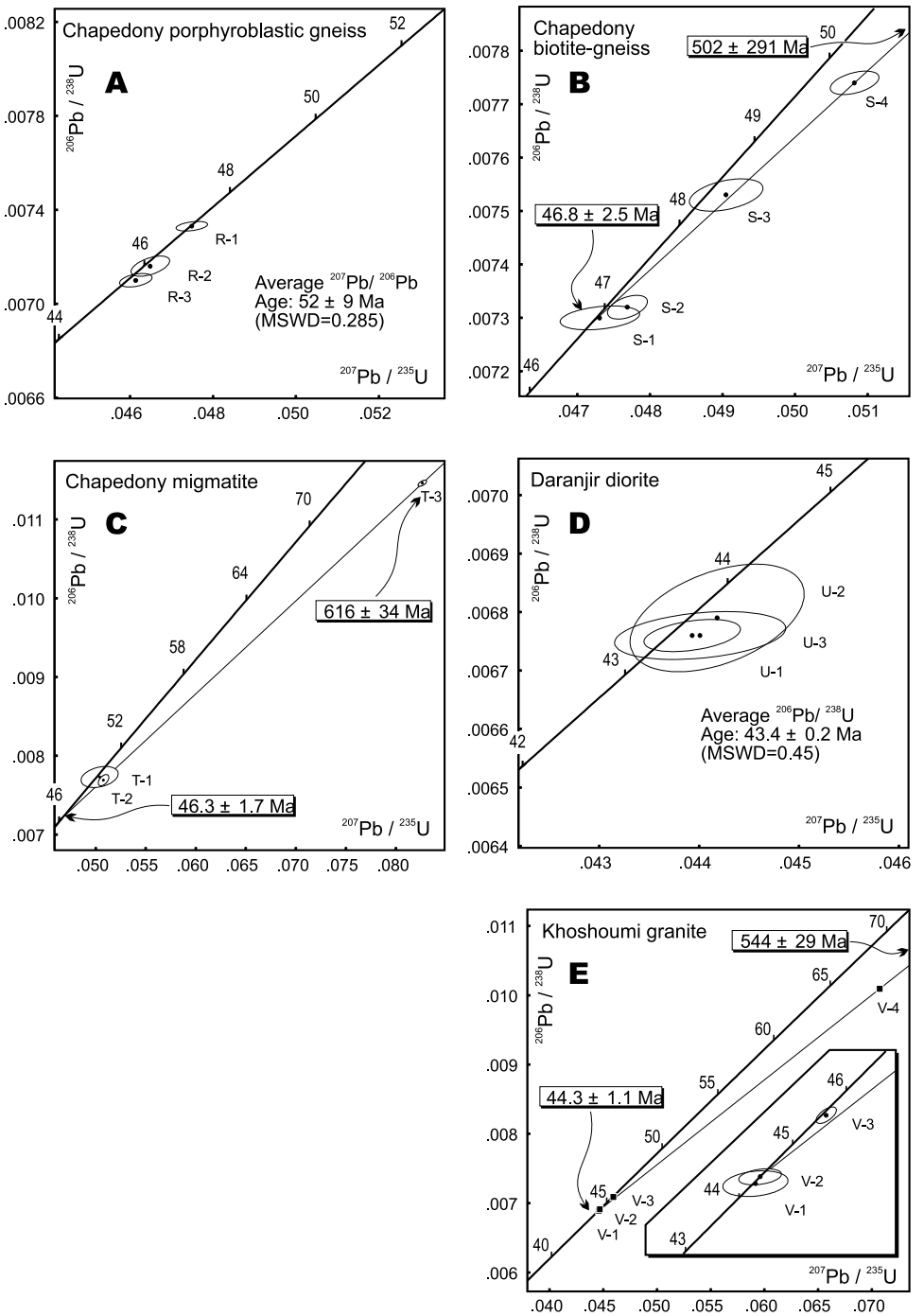

Fig. 8. Concordia diagrams for the Cenozoic rocks of the Saghand area.

method, following the procedures described in Couture and others (1993) and Couture and Dymek (1996). Measurement of major and trace elements was performed on fused lithium metaborate glass discs and pressed-powder pellets, respectively, using a Siemens SRS 200 X-Ray Fluorescent Spectrometer equipped with Rh tube at Washington University. Concentrations of Cr, Co, Sc, Cs, Ba, Ta, Hf, Ti, Th, U and the rare earth elements (REE) were determined by instrumental neutron activation analysis (INAA), following the procedures described in Korotev (1987, 1991). Samples were irradiated in the University of Missouri-Columbia research nuclear reactor and were measured using gamma-ray spectrometers equipped with Ge detectors at Washington University.

The results of major and trace element analyses are listed in table 2. The FeO and Fe_2O_3 concentrations are recalculated from Fe_2O_3* (total iron as Fe_2O_3 measured by XRF), using recommended Fe_2O_3/FeO ratios of Middlemost (1989). Also, the expected concentrations of Gd (Gd*) and Pr (Pr*), not measured by INAA, are extrapolated from the chondrite-normalized concentrations of other REE, assuming linear trends.

Interpretation of Geochemical Data

Cambrian Granitoid Suite (CGS).—Samples of the CGS (for example, Ariz Granodiorite) range from Al-saturated to metaluminous (fig. 9A). They are classified consistently as monzogranite and granodiorite based on the normative alkali-feldspar-quartz-plagioclase (AQP) and Ab-An-Or classification schemes (fig. 9B and 9C). The chondrite-normalized, extended, trace element plot of the CGS (fig. 10A) displays variably fractionated REE patterns ($[La/Yb]_N$ = 7.4 to 18.4) coupled with negative Eu anomalies (Eu/Eu* = 0.43 to 0.59), which reflect magmatic differentiation involving plagioclase fractionation.

An important geochemical feature of the CGS rocks is the underabundance of high-field-strength elements (HFSE) Nb and Ta, and the overabundance of large-ion-lithophile element (LILE) Th, with respect to the light rare earth elements (LREE), as compared to the chondritic concentrations. These are reflected in their $(Nb/La)_N$ and $(Th/La)_N$ ratios that range from 0.1 to 0.2, and from 2.1 to 4.4, respectively. The coupled negative Nb (and Ta) and positive Th anomalies in magmatic rocks (despite similar bulk distribution coefficients of these elements), is considered a chemical signature of a subduction-zone component introduced at destructive plate boundary settings.

Comparison between the trace element patterns of CGS rocks (fig. 10A) and those of the Jurassic quartz-monzodiorites and granites of the Palisade Crest Intrusive Suite (Sawka and others, 1990; fig. 10C), part of the Sierra Nevada Batholith of the western North American continental margin, reveals remarkable similarities between the two suites. Prominent and comparable LREE enrichments, negative Nb-Ta anomalies and elevated Th abundances characterize the trace element patterns of both plutonic suites. These and comparisons with other orogenic plutons of present-day active marginal settings (Ramezani, ms, 1997) substantiate the origin of the CGS magma as a continental-margin arc setting.

Boneh-Shurow Granitic Gneisses (BSG).—Pink, quartzofeldspathic gneisses of the Boneh-Shurow Complex are interpreted to have originated from a suite of intrusive dikes and sills of granitic composition which underwent lower-amphibolite facies metamorphism (about 547 Ma) shortly after their emplacement (see above). The BSG samples are fairly uniform in composition, highly silicic (71.7 to 77.7 wt% SiO_2) and in general are slightly metaluminous (fig. 9A). They plot consistently in the monzogranite and granodiorite fields on the AQP diagram (fig. 9B). The chondrite-normalized trace element plot of the BSG (fig. 10B) displays variably fractionated REE [$(La/Yb)_N$ = 4.1 to 15.6)] along with negative Eu anomalies (Eu/Eu* = 0.3 to 0.68),

TABLE 2

Geochemical data for representative rocks of the Saghand area

SAMPLE	JR95-G54	JR95-G55	JR94-G14	JR95-G39	JR94-G7	JR95-G42	JR94-G8	JR95-G49	JR94-G28	JR95-G47
Rock[1]	Gd	Granite	Gd	Granite	Gneiss	Gneiss	Gneiss	Gneiss	Rd	Dacite
Unit	CGS	CGS	CGS	CGS	BSG	BSG	BSG	BSG	CVSU	CVSU
SiO2[2]	68.81	76.26	65.91	76.15	71.72	75.38	75.37	77.74	79.06	67.05
TiO2	0.52	0.16	0.69	0.18	0.34	0.18	0.09	0.13	0.24	0.81
Al2O3	14.56	12.57	14.57	12.68	13.17	12.36	12.63	11.71	11.95	13.23
Fe2O3[3]	4.19	1.54	4.54	1.47	2.06	1.79	1.23	1.36	0.15	7.21
MnO	0.06	0.01	0.06	0.02	0.02	0.02	0.02	0.01	0.01	0.05
MgO	1.40	0.25	2.10	0.17	0.46	0.37	0.06	0.15	0.19	0.74
CaO	3.57	1.06	3.43	0.48	1.27	1.41	1.25	0.93	0.45	1.76
Na2O	3.58	3.47	3.03	4.22	3.84	4.48	3.63	3.66	6.22	6.48
K2O	2.86	4.51	4.21	4.92	4.41	2.75	4.77	3.81	1.46	1.70
P2O5	0.08	0.01	0.16	0.01	0.11	0.05	0.02	nd	0.08	0.21
LOI	0.62	0.41	1.41	0.39	0.70	1.45	1.24	0.36	0.57	0.93
Total	100.24	100.24	100.11	100.71	98.10	100.23	100.31	99.84	100.38	100.15
Cr[4]	18	2	(75)	1	6	(10)	3	nd	2	1
Ni	9	nd	22	nd	4	4	nd	nd	4	nd
Co	8	2	(11)	3	3	(4)	1	1	10	3
Sc	13	3		3	6		2	5	3	11
V	70	10	82	5	19	5	9	nd	6	14
Zn	38	12	64	16	14	21	4	26	2	19
Sn	4.20	5.30	8.30	3.00	7.30	3.40	3.30	3.80	5.90	14.30
Rb	83	114	131	51	152	49	126	70	18	16
Cs	1.83	1.05		0.23	2.93		0.49	0.26	0.07	0.15
Ba	868	648	(644)	659	648	(798)	658	995	154	205
Sr	171	77	184	38	103	45	168	78	26	56
Ga	17	13	16	15	17	15	12	14	7	29
Ta	0.49	0.93		0.30	1.34		0.86	0.81	0.38	1.55
Nb	7.4	7.6	15.7	2.9	11.5	9.0	6.3	8.5	2.4	22.7
Hf	5.89	4.75		7.15	8.25		2.93	5.36	3.53	23.00
Zr	200	118	262	191	226	161	80	146	125	850
Ti	3141	947	4155	1097	2044	1079	546	755	1433	4844
Y	27	24	25	14	39	27	11	42	26	114
Th	8.61	18.36		13.32	15.38		19.19	16.29	5.82	8.41
U	0.97	3.64		1.93	3.01		4.55	4.18	2.32	2.37
La	34.40	34.00		44.80	31.90		30.90	39.90	30.20	57.80
Ce	67.20	62.50		88.40	71.00		51.70	83.60	57.20	135.20
Pr*	7.51	6.28		9.44	8.10		4.58	9.07	6.28	16.69
Nd	27.30	20.50		32.80	30.10		13.20	32.00	22.40	67.00
Sm	5.59	3.92		4.97	7.22		2.18	7.75	4.06	17.82
Eu	1.06	0.55		0.70	0.92		0.42	0.76	0.89	3.92
Gd*	5.37	3.88		3.65	7.57		1.63	7.81	4.22	20.10
Tb	0.82	0.60		0.49	1.21		0.22	1.23	0.67	3.34
Yb	2.80	3.12		1.65	5.25		1.34	4.89	2.47	13.70
Lu	0.40	0.47		0.25	0.75		0.22	0.71	0.36	2.05
Eu/Eu*	0.59	0.43	-	0.50	0.38	-	0.68	0.30	0.65	0.63

reflecting magmatic fractionation. Similar to that in the CGS rocks, the negative Nb-Ta and positive Th anomalies [$(Nb/La)_N = 0.2$ to 0.4, $(Th/La)_N = 3.3$ to 5.1] in the BSG are characteristic of destructive plate margin magmas.

Cambrian Leucogranite Suite (CLGS).—Shallow-intrusive, leucocratic rocks of the Zarigan and Douzakh-Darreh intrusions are highly silicic (SiO_2 wt% = 74.6-77.7) and are Al-saturated (to slightly peraluminous, fig. 9A). They tend to plot within or near the tonalite field on the AQP diagram, whereas the Ab-An-Or classification scheme

TABLE 2
(continued)

SAMPLE	JR94-G1	JR94-G3	JR95-G38	JR94-G16	JR95-A40	JR95-G37	JR94-G17	JR95-G50	avg. error
Rock	Tj	Tj	Tj	Gd	Granite	Gd	Granite	Granite	1 sigma (%)
Unit	CLGS	CLGS	CLGS	TGS	TGS	TGS	TGS	TGS	
SiO2	74.67	74.58	77.68	71.31	73.93	73.30	75.77	71.81	0.35
TiO2	0.39	0.31	0.17	0.32	0.25	0.28	0.02	0.31	3.23
Al2O3	14.99	14.77	12.17	14.65	13.01	13.41	13.35	14.09	0.93
Fe2O3*	0.72	0.78	0.70	3.00	2.48	2.88	1.08	2.99	0.98
MnO	0.01	0.01	0.03	0.04	0.06	0.05	0.05	0.07	11.83
MgO	0.10	0.12	0.27	0.57	0.41	0.64	0.09	0.63	3.24
CaO	0.37	0.84	1.02	1.92	1.36	1.29	0.70	2.24	1.65
Na2O	8.47	7.16	5.26	3.87	3.37	3.69	3.57	3.01	3.18
K2O	0.23	1.09	1.30	3.23	3.97	3.32	4.52	3.96	3.17
P2O5	0.03	0.04	0.02	0.09	0.05	0.09	0.02	0.11	17.71
LOI	0.41	0.57	1.52	1.11	0.97	1.42	0.53	0.67	
Total	100.40	100.26	100.13	100.11	99.85	100.36	99.72	99.89	
Cr	4	4	6	2	2	2	(8)	3	1.58
Ni	3	3	4	2	nd	nd	6	nd	44.16
Co	nd	1	nd	4	3	3	nd	4	0.99
Sc	nd	1	1	6	5	7		5	0.95
V	7	7	4	25	17	25	nd	15	10.99
Zn	6	9	nd	50	42	24	42	61	8.2
Sn	0.70	2.40	nd	7.90	5.00	4.70	6.70	4.90	71.43
Rb	4	20	35	117	153	121	163	162	8.23
Cs	0.07	0.31	0.23	7.61	6.86	1.70		6.29	2.73
Ba	78	341	61	732	502	602	(447)	787	1.99
Sr	74	172	25	152	84	140	51	221	0.94
Ga	20	16	14	18	14	16	17	14	7.45
Ta	0.63	0.59	0.93	0.80	1.07	0.91		1.24	2.18
Nb	6.2	5.1	7.2	10.4	10.8	8.8	12.7	15.6	8.94
Hf	8.74	7.65	7.91	4.48	4.34	4.32		4.68	1.12
Zr	252	224	172	147	132	122	66	165	0.96
Ti	2314	1888	992	1936	1475	1667	126	1846	3.23
Y	2	3	29	16	22	21	34	16	6.6
Th	1.92	1.44	26.90	12.29	17.55	12.32		24.00	1.02
U	0.86	0.89	4.58	2.21	3.36	2.92		2.65	7.69
La	2.72	5.55	1.96	34.30	32.60	26.80		57.80	0.98
Ce	3.62	6.83	2.96	64.20	63.70	50.10		113.60	1.06
Pr*	0.30	0.60	0.32	6.48	6.68	5.32		11.85	
Nd	0.80	1.70	1.15	21.30	22.80	18.40		40.20	4.56
Sm	0.14	0.23	0.48	4.08	4.58	3.96		6.56	1.61
Eu	0.20	0.53	0.11	0.77	0.59	0.66		1.13	1.12
Gd*	0.15	0.24	1.38	3.42	4.15	3.91		4.30	
Tb	0.02	0.04	0.37	0.49	0.62	0.61		0.55	4.23
Yb	0.44	0.47	5.56	1.54	2.14	2.36		1.49	1.51
Lu	0.08	0.09	0.87	0.24	0.31	0.34		0.23	2.14
Eu/Eu*	4.18	6.77	0.42	0.63	0.41	0.51		0.65	

NOTES: [1] Gd = granodiorite; Rd = rhyodacite; Tj = trondhjemite.
[2] Major oxide concentrations in percent.
[3] Total Fe measured as Fe_2O_3 after complete oxidation of iron by ignition in furnace.
[4] Trace element concentrations in parts per million.
* Extrapolated concentrations from chondrite-normalized concentrations of other rare earth elements assuming linear trends.
nd = not detected; ( ) = XRF value where INAA analysis not available.

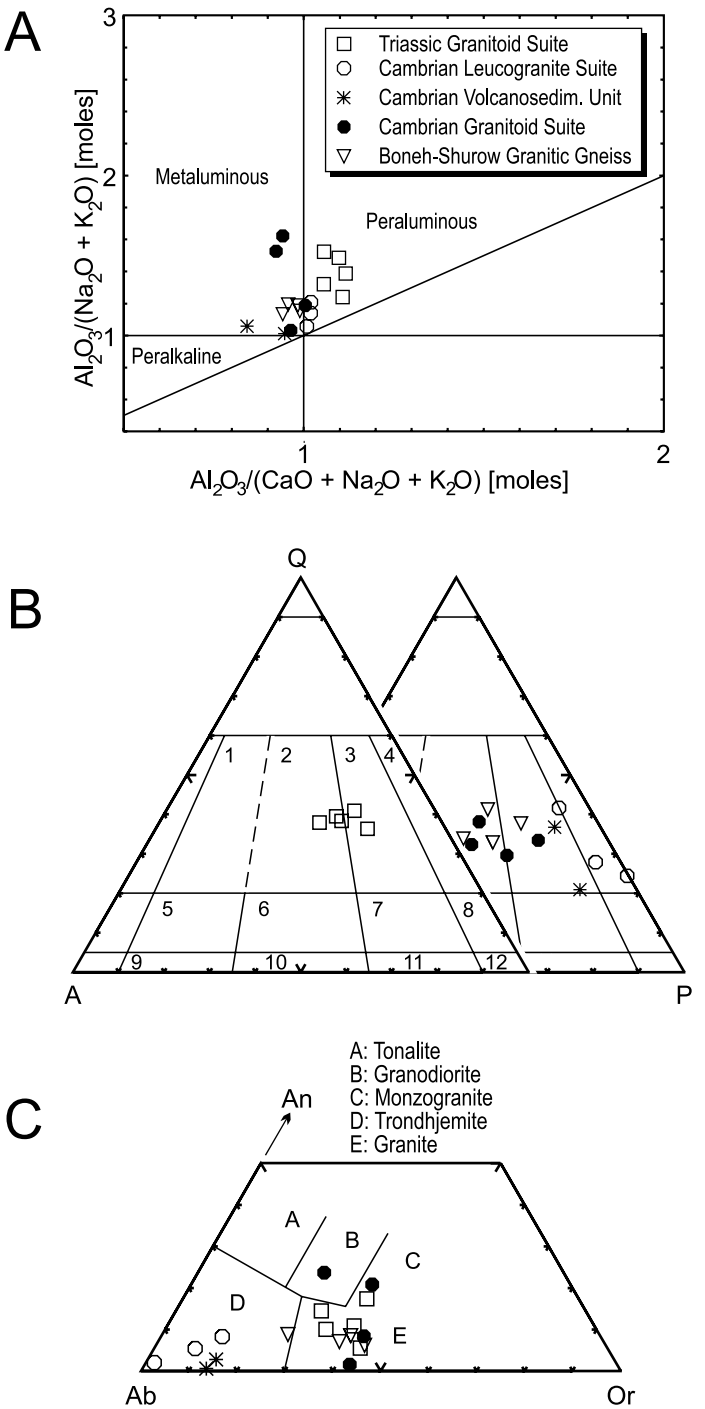

Fig. 9. Major element diagrams for the investigated magmatic rocks of the Saghand area. (A) Alumina-saturation plot after Shand (1943). (B) Quartz - alkali-feldspar - plagioclase (QAP) classification after Le Maitre (1989). (C) Ab-An-Or normative classification after Barker (1979).

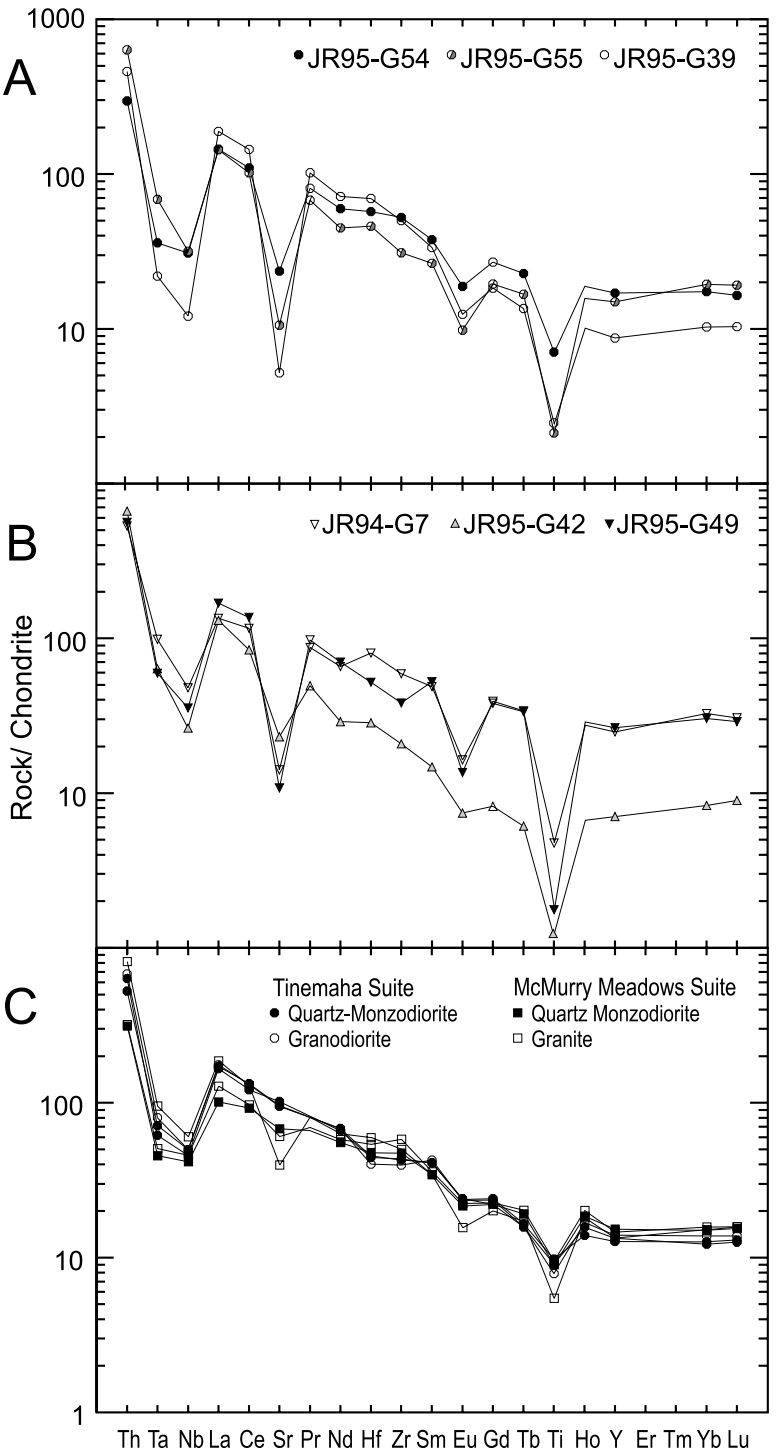

Fig. 10. Extended chondrite-normalized trace element plots for the igneous rocks of the Cambrian Granitoid Suite (A), Boneh-Shurow Gneiss (B) and the Palisade Crest Intrusive Suite (C).

clearly distinguishes these rocks as trondhjemites (fig. 9C). The trondhjemitic character of the CLGS rocks is consistent with their plagioclase-dominated mineralogy, Na-rich and K-poor chemistry and their normative corundum contents (0.20% to 0.32%).

The CLGS trondhjemites are characterized by rare, concave-up, REE patterns on the chondrite-normalized plot (fig. 11A). These patterns reflect a prominent depletion in middle REE (MREE) relative to LREE and HREE that are not readily explained by simple fractionation or magma mixing models. In fact, positive Eu anomalies in the Zarigan trondhjemites (Eu/Eu* = 4.18 to 6.77) are suggestive of plagioclase accumulation in the magma. The large positive Zr and HF anomalies in the CLGS patterns, despite moderate Zr and Hf concentrations in these rocks (table 2), are further evidence for a significant MREE depletion in their source magma. Despite the general similarity in trace element patterns, the Douzakh-Darreh trondhjemite (sample JR95-G38) appears to be more enriched in HREE compared to those of the Zarigan intrusion.

Cambrian Volcano-Sedimentary Unit (CVSU).—The dominantly felsic to intermediate volcanic rocks of the CVSU are too diverse in lithology to allow a statistically valid compositional analysis based on our limited sample set. Nevertheless, the major element compositions of the CVSU rhyodacite and dacite-porphyry show many similarities to those of the CLGS trondhjemites (fig. 9A to 9C). Though clearly dacitic in mineralogy, the Ab-An-Or classification identifies the CVSU rocks as trondhjemite and distinguishes them from the common calc-alkaline dacites (fig. 9C).

The trace element compositions of the CVSU samples are more closely associated with the CGS, rather than the CLGS. The chondrite-normalized plot of these rocks (fig. 11B) displays variable degrees of fractionation [$(La/Yb)_N$ = 2.9 to 8.3] which is more pronounced in the rhyodacite. Both rocks exhibit negative Nb-Ta and slightly positive Th anomalies [$(Nb/La)_N$ = 0.1 to 0.4, $(Th/La)_N$ = 1.2 to 1.6], typical of subduction-derived magmas.

Triassic Granitoid Suite (TGS).—Representative samples of the Late Triassic Chamgoo, Anarg and Esmailabad granitoid intrusions are distinguishably peraluminous (fig. 9A) and corundum-normative (Co wt% = 0.75 to 1.56). Most samples plot close to the monzogranite-granodiorite boundary on the AQP diagram (fig. 9B). The fractionated trace element patterns of the TGS rocks [$(La/Yb)_N$ = 7.7 to 26.3, (fig. 11C)] are comparable to those of the CGS, in terms of both Eu anomalies ((Eu/Eu* = 0.41 to 0.65) and combined Nb-Ta-Th anomalies [$(Nb/La)_N$ = 0.3, $(Th/La)_N$ = 2.9 to 4.4]. Nevertheless, the average Rb and Cs contents of the TGS magmas are noticeably higher compared to those of the CGS (table 2).

DISCUSSION

Neoproterozoic Clastic Sedimentation

The oldest documented and isotopically dated rocks in the Saghand region (and probably the entire area) of central Iran belong to the Tashk Formation. The depositional age of the formation is constrained between 627 Ma, the U-Pb age of the youngest concordant (detrital?) zircon found in a tuffaceuos rock, and 533 Ma. The latter is the zircon age of the oldest known magmatic intrusion (Ariz Granodiorite) into the formation. Accordingly, an overall Late Neoproterozoic to Early Cambrian age is assigned to the Tashk Formation. Considering its large thickness, at least a portion of the formation is likely to have been deposited during the latest Neoproterozoic.

Based on its lithology and rock facies, the Tashk Formation must have been deposited in a marginal marine (outer shelf-slope) environment, adjacent to centers of basaltic and/or pyroclastic eruption. Although the geographic extent of the Tashk Formation is by definition limited to the Saghand area, its correlative successions are

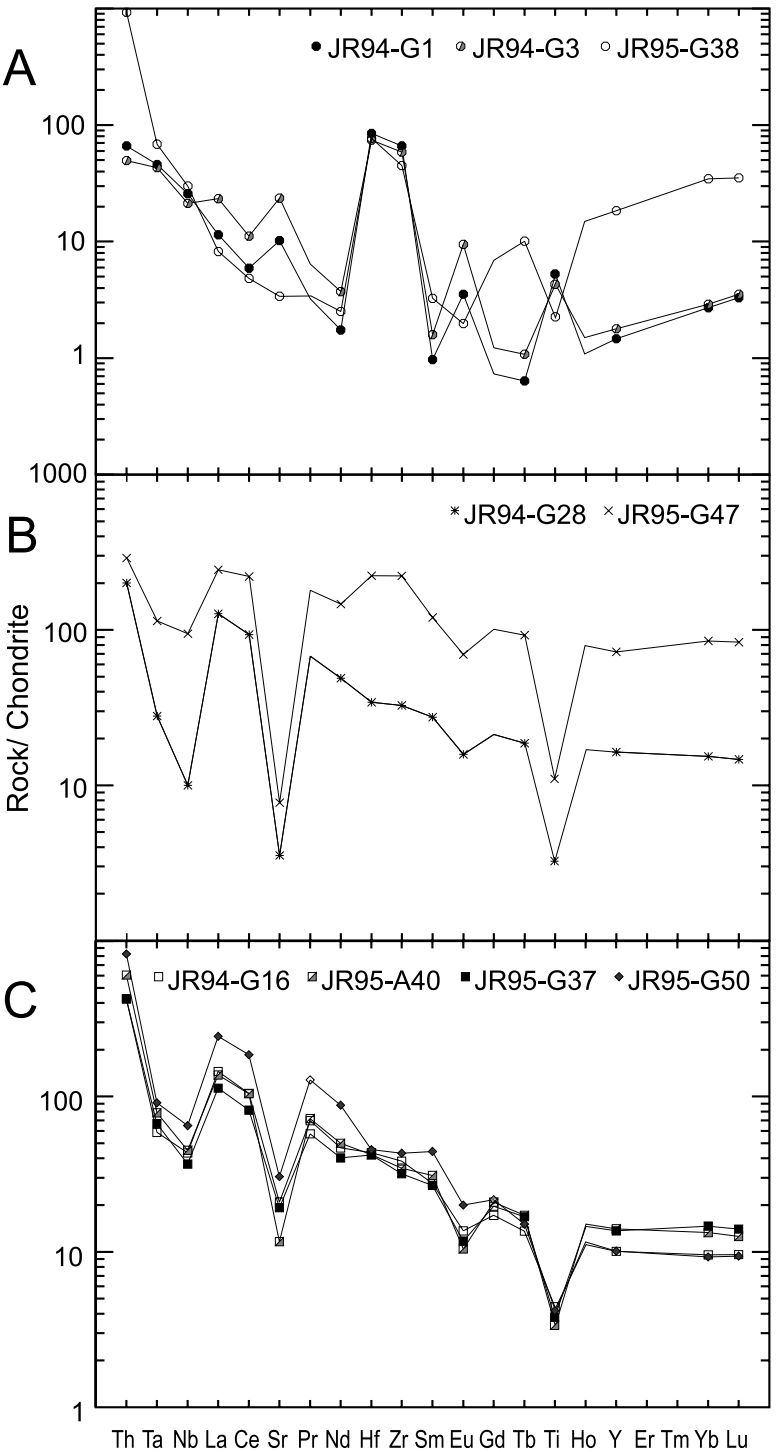

Fig. 11. Extended chondrite-normalized trace element plots for the igneous rocks of the Cambrian Leucogranite Suite (A), Cambrian Volcano-Sedimentary Unit (B) and the Triassic Granitoid Suite (C).

recognized (or suspected) throughout the central Iran-Alborz province. These include the Morad Series (Huckriede and others, 1962), Kalmard Formation (Stöcklin, 1968) and the Upper Taknar Formation (Müller and Walter, 1984) throughout the Kashmar-Kerman Tectonic Zone (fig. 2), and the Kahar Formation (Dedual, 1967) in the central Alborz Mountains. In addition, unclassified strata of graywackes and slates that are known to underlie the lower Paleozoic successions elsewhere in central Iran (for example, Yazd area) and in Northwest Iran (Azerbaijan) are possible correlatives for the Tashk Formation. These imply that the Tashk "facies" is widely distributed throughout the Iranian Plateau and is likely to underlie Phanerozoic platform strata at depth in many locations.

Early Cambrian Arc Magmatism

Arc Plutonism.—One of the key outcomes of this study was the identification of granite-tonalite intrusions of the Cambrian Granitoid Suite (CGS) in the Saghand region, and central Iran, in general. The CGS rocks produced fairly precise Early Cambrian crystallization ages of approximately 533 Ma, somewhat younger than their previously assumed Precambrian age. A marginal arc setting is proposed for the CGS, based on its geochemical characteristics and country-rock facies (Tashk Formation).

The interpreted crystallization age of the Boneh-Shurow granitic orthogneiss (BSG), 542 ± 9 Ma, overlaps within uncertainty with the emplacement age of the CGS. Taking into account the magmatic-arc affinity of the BSG magma, it can be inferred that the CGS and BSG belong to a similar magmatic episode that probably started in the latest Neoproterozoic and continued into the Early Cambrian. Nevertheless, the conspicuous metamorphic facies and structural setting of the Boneh-Shurow Complex places the BSG in a very different tectonic environment than the CGS. This environment can be interpreted as the distal part of a late Neoproterozoic-Early Cambrian magmatic arc complex, in which the terrigenous, semi-pelitic and carbonaceous protoliths of the Boneh-Shurow complex were progressively deformed, metamorphosed, and simultaneously injected by granitic magmas ascending through the crust. At the shallower levels of the arc complex, the Tashk Formation was intruded by the CGS plutons, both remaining essentially unmetamorphosed.

The metamorphic rocks of the Boneh-Shurow Complex crop out in the vicinity of Bafq (Gneise von Bafq of Huckriede and others, 1962), to the south of our study area (fig. 2). At least parts of the Narigan Granite (for example, its biotite-granite facies) in the Bafq area might be correlated with the CGS. The "crystalline basement" orthogneisses and mica-schists of the Zebar-Kuh Range (Sahandi and others, 1984) to the northeast of the Saghand area are also possible correlatives of the Boneh-Shurow Complex. The mica-schist and phyllites of this area were intruded by two large intrusions, Sarhangi and Robat Granites, which are disconformably overlain by Cambrian (and younger) strata and are likely to be the product of Early Cambrian arc plutonism. The Bornanvard Intrusion (see for example, Müller and Walter, 1984) which is emplaced into the late Neoproterozoic Taknar Formation within the Taknar Inlier of the Kashmar-Kerman Tectonic Zone (fig. 2) is another possible correlative of the CGS plutons. Crawford (1977) determined a Rb-Sr model age of approximately 540 Ma for the Bornavard Granite that, although imprecise, supports the above correlation.

Despite the abundance of candidates for the Early Cambrian arc plutons throughout the Kashmar-Kerman Tectonic Zone, no other intrusion that can be reliably attributed to this event has, to the authors' knowledge, been documented from elsewhere in central Iran. This observation suggests that the tectonic zone may embody the remnants of an Early Cambrian magmatic arc. Alternatively, this spatial distribution of arc plutons could be merely the result of poor exposure of the platform basement elsewhere, and hence may not be of any tectonic significance.

Arc Volcanism.—The Early Cambrian arc plutonism in the Saghand region was followed rather uninterruptedly by the predominantly felsic to intermediate volcanism of the Cambrian Volcano-Sedimentary Unit (CVSU) at approximately 528 Ma. Geochemical evidence from the few available CVSU felsic volcanic samples suggests a magmatic-arc setting for this volcanic episode.

The CVSU has been generally regarded as the Infracambrian (Eocambrian) unit in the Saghand region (Haghipour and Pelissier, 1977), whereas its widespread equivalents throughout central Iran are referred to by the general term Rizu-Desu Series (see for example, Berberian and King, 1981). The extensive, felsic volcanic-dominated Esfordi Formation (Förster and Borumandi, 1971) is a well-documented equivalent of the CVSU (or Rizu-Desu Series) in the Bafq area (fig. 2). The Pb-Pb isochron ages of a syn-sedimentary orebody within this formation (595 to 760 Ma ± 120 Ma, Huckriede and others, 1962), though highly ambiguous, were long considered as evidence for the Precambrian age of the basement rocks in Iran (Stöcklin, 1968). The U-Pb zircon age of 528.2 ± 0.8 Ma for the basal rhyodacite flow in the Douzakh-Darreh Mountain clearly indicates an Early Cambrian age for the CVSU and its equivalents in central Iran. Lithologically similar basal flows have been reported from other successions of the Rizu-Desu Series (see for example, the Zebar-Kuh Range: Sahandi and others, 1984) and are likely to have a similar age.

Late-stage Trondhjemite Intrusion.—The CVSU arc volcanism was coincident with, and followed by, massive, shallow-level, felsic intrusions of the Cambrian Leucogranite Suite (CLGS) at 525 ± 7 Ma. The geochemical results of our study identify these intrusions as trondhjemite, with major element compositions largely comparable to those of the CVSU felsic volcanic rocks. However, the chondrite-normalized trace element patterns of the CLGS rocks are distinct from the typical arc-related magmas.

Modern petrologic models have linked the generation of trondhjemitic melts to the subduction of young (<25 Ma), hot oceanic lithosphere in the Archean to modern island- and continental-arc settings (Drummond and Defant, 1990; Drummond and others, 1996). Accordingly, the high-pressure melting of (metamorphosed) oceanic crust under garnet-amphibolite to eclogite conditions at depths of 75 to 85 kilometers can produce magmas of tonalite-trondhjemite-dacite (TTD) compositional character. In addition, the concave-up REE patterns of many trondhjemite suites is attributed to hornblende-melt fractionation and the strong affinity of this mineral for MREE (Drummond and Defant, 1990). Overall, the geochemical characteristics of the CLGS trondhjemites, as well as their spatial and temporal relationships to other magmatic suites in the area, are consistent with the model of TTD generation at convergent plate boundaries (Ramezani and others, 1999). The intrusion of CLGS plutons marks the termination of the late Neoproterozoic-Early Cambrian arc magmatism in central Iran.

Late Triassic Plutonism

Our new U-Pb zircon data constrain the emplacement age of the Esmailabad Granite at 218 ± 3 Ma, the Norian stage of Late Triassic. They also demonstrate that the Late Triassic granite-tonalite plutons of the Saghand region are more widespread than previously recognized and include such intrusions as the Chamgoo Granodiorite. Although the Triassic intrusions are generally comparable in chemistry to the Early Cambrian igneous suites (for example, CGS), their distinguishably peraluminous character, as well as their higher abundances of LILE (Rb and Cs), suggest substantial involvement of sialic material in their origin. Based on the limited available data, these intrusions may thus be interpreted as anatectic or collisional granitoids.

Magmatic intrusions of Late Triassic age are uncommon in central Iran and appear to be absent from the Kashmar-Kerman Tectonic Zone, beyond the boundaries of the Central Lithotectonic Domain. Unknown spatial distribution, as well as the absence of associated volcanic or metamorphic rocks, render the origin of these rocks

enigmatic. Nevertheless, the occurrence of these intrusions is fairly consistent with the Mesozoic geologic evolution of central Iran.

The Mesozoic stratigraphic record of the central Iran-Alborz province is characterized by a major unconformity in the Upper Triassic. Regardless of a few exceptions, the lagoonal-terrestrial siliciclastic sediments of Rhaeto-Liassic age, which are known in the Main Alborz as the coal-bearing Shemshak Formation, overlie unconformably the Lower Triassic or older strata throughout the province. This unconformity has been attributed by various authors to the Early Alpine (Berberian and King, 1981), Early Kimmerian (Davoudzadeh and Schmidt, 1984) or the Cimmerian (Şengör, 1987) orogenic event. The newly recognized occurrence of Late Triassic intrusions in the Saghand region is in accord with the above notion, providing further evidence for a Late Triassic tectonomagmatic episode of possible collisional character. Further investigations are necessary to decipher the trend and regional extent of the late Triassic collisional orogeny.

Tertiary Metamorphism and Post-kinematic Intrusions

Historically, the metamorphic rocks of the Chapedony Complex have played a pivotal role in the hypotheses regarding the origin of continental crust in the Middle East region. Recognized as the most intensely metamorphosed rock unit in the polymetamorphic Saghand - Poshteh-Badam region, the Chapedony complex was visualized to represent the Precambrian basement of the Iranian plateau (Hushmandzadeh, ms, 1969; Haghipour and Pelissier, 1977) and was commonly correlated with the Pan-African metamorphic terranes of the Arabian-Nubian Shield. Accordingly, it has been widely stated that the consolidation of the basement throughout the Iranian plateau took place by metamorphism and anatexis at about 1000 to 600 Ma (Stöcklin, 1974; Berberian and King, 1981; Davoudzadeh and others, 1986).

Our multiple U-Pb zircon ages measured from various rock types of the Chapedony Complex identify this unit unmistakably as a Tertiary (Middle Eocene) metamorphic complex, with peak metamorphism at approximately 46 Ma. The latter was followed by late- to post-metamorphic intrusion of granite-diorite plutons into the complex at approximately 45 Ma. The reproducibility and consistency of our measured ages among the high-grade gneisses, migmatites and the post-kinematic intrusions rule out the possibility of a young (Eocene) overprint on an old (Precambrian) metamorphic complex, as an alternative interpretation. The new data necessitate a reinterpretation of the Chapedony Complex and its tectonic significance, in the context of the Cenozoic geology of central Iran.

The Eocene epoch marks the wane of a long period of marine sedimentation and the onset of widespread arc magmatism associated with the early Alpine Orogeny in the Central Iran-Alborz Province. Predominantly andesitic volcanism and granitic plutonism occurred largely along the Urmieh-Dokhtar magmatic arc, and to a lesser extent, throughout the interior of the province. This vast episode of orogeny was the result of convergence between the Arabian plate (Gondwana) and the Iranian plateau, and the closure of the Tethys oceanic tract(s) by subduction. The metamorphism/anatexis of the Chapedony Complex appears to be concomitant with these Alpine orogenic activities and can be regarded as the deep-seated manifestation (or source) of the Eocene magmatism at or near the surface. Metamorphic complexes comparable in age and setting to the Chapedony Complex are widely distributed throughout the Alpine orogenic belt of Europe (Coward and Dietrich, 1989).

Regional Implications of the Late Neoproterozoic-Early Cambrian Orogeny in Iran

The commonly accepted reconstructions of the continents in the Late Neoproterozoic (see for example, Powell and others, 1980; Lawver and Scotese, 1987; DeWit and others, 1988; McKerrow and others, 1992; Unrug, 1997), invariably place the Indian

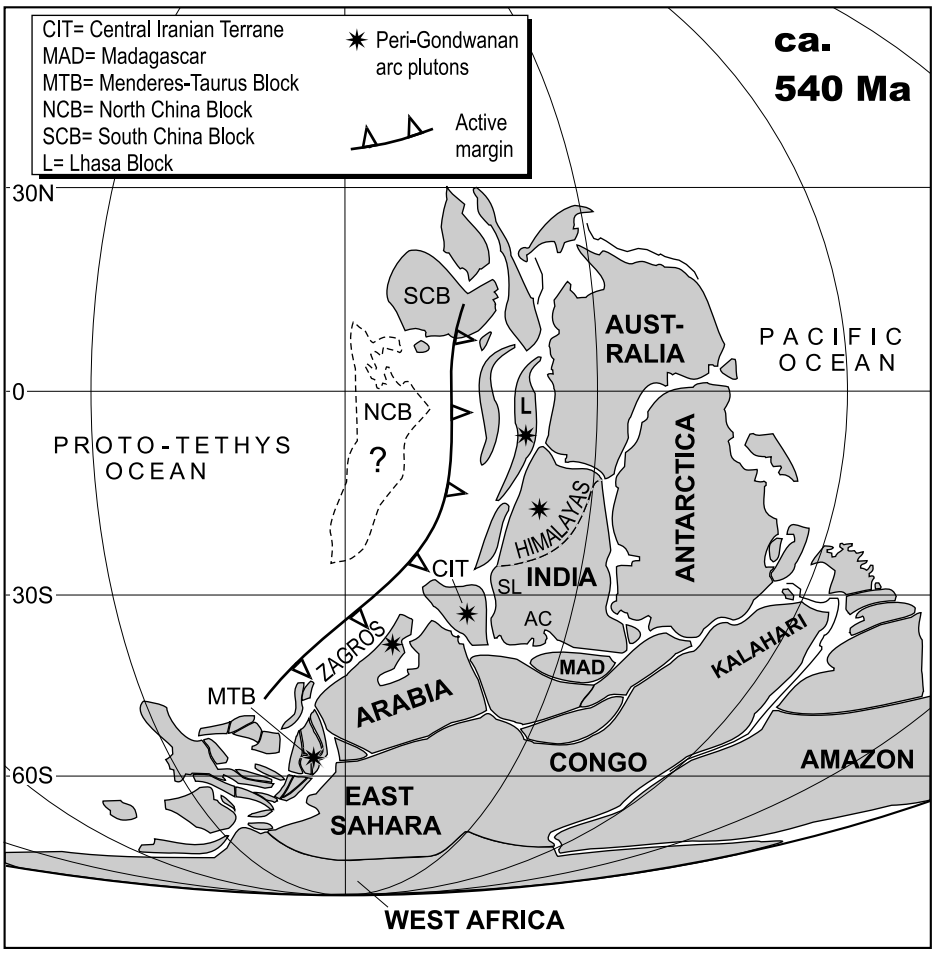

Fig. 12. Gondwanaland reconstruction in Early Cambrian based on Molleweide projection of tectonic plates at 540 Ma by the PLATES Project (1999), with modifications based on C. Scotese (personal communication, 2000) and the results of this work. Precambrian cratons in bold letters. Other abbreviations: AC = Aravalli Craton, SL = Salt Range.

continent adjacent to the eastern margin of Africa and its Arabian subplate, as part of the larger Gondwanaland supercontinent (see fig. 12). Taking into account the necessary edge fits among the Gondwanan fragments, the plate reconstructions yield a gap of significant width between the western Indian (Salt Range) and the eastern Arabian (Oman) margins. Regional stratigraphic and paleomagnetic constraints implicate this gap as the most likely site for the Central Iranian Terrane within the Late Neoproterozoic Gondwanaland assembly.

The common distribution of the Early Cambrian evaporite-carbonate facies among central Iran (CVSU, Rizu-Desu Series), Zagros (Hormuz Formation), Oman (Ara Formation) and Salt Range of Pakistan (Punjab Saline Series) points to the geographic continuity of these regions in the Early Cambrian (Husseini, 1989; Talbot and Alavi, 1996). The possible correlation of the underlying late Neoproterozoic clastic sequences in Iran (Tashk Formation), Oman (Huqf Group) and the Lesser Himalaya (Purana Sequence), as well as the overall uniformity of the Lower Paleozoic

platform successions in the above regions, provide further support for the Arabia-Iran-India continuity (Ramezani, 1996). The paleomagnetic work of Becker and others (1973) and Soffel and Förster (1981) yielded Eocambrian geomagnetic pole positions for central Iran which are fairly similar to those from rocks of comparable age on the Indian continent, suggesting that central Iran and Northwest India were located at about the same paleolatitude by the end of the Proterozoic Era. These lines of evidence collectively favor the placement of the Central Iranian Terrane alongside the Arabian and Indian plates, along the Proto-Tethyan margin of the Neoproterozoic Gondwanaland (fig. 12).

The 548 to 526 Ma orogeny in central Iran brings about significant paleotectonic implications, in the context of the Arabia-Iran-India paleogeographic continuity. If the late Neoproterozoic-Early Cambrian events in central Iran were associated with the establishment of a continental-margin (Andean-type) magmatic arc, the adjoining Arabian and Indian (Proto-Tethyan) margins of the Gondwanaland must have experienced a comparable set of events. The verification of this hypothesis is an arduous task, mainly because of the complex Phanerozoic history of the above margins. The Proto-Tethyan margin of India has been intensely affected by the Cenozoic Himalayan Orogeny, whereas the ancient rocks of the Arabian margin are buried under the thick sedimentary piles of the Arabian Platform and the Zagros Basin. In the following discussion we attempt to demonstrate, based on available geologic and age data, the evidence for concurrent orogenic activity in various Peri-Gondwanan segments of the Proto-Tethys margin.

The Himalayan Segment.—Evidence for a Late Precambrian to Cambro-Ordovician orogeny has been established from three major tectonic subdivisions of the Himalayas; namely the Lesser, the Higher (Greater) and the Tethys (Tibetan) Himalayan zones (Mehta, 1977; Garzanti and others, 1986; Baig and others, 1988). The evidence includes the record of Himalayan sedimentary sequences, as well as magmatic intrusions of Neoproterozoic-Cambrian age, such as the well-known approximately 545 Ma Mandi Granite (Jäeger and others, 1971; Mehta, 1977). The overprinting effects of the Cenozoic Himalayan deformation and metamorphism have traditionally hampered the study of these rocks, leading to debates over their origin and tectonic significance.

Bodies of augen-gneiss and gneissic porphyritic granite of Cambrian age occur throughout the Himalayan province and have been identified as far north as Tibet. A 1700 kilometer long belt of peraluminous granitoids plutons within the crystalline nappes of the Lesser Himalaya has yielded Rb-Sr whole rock (and limited U-Pb) ages that range between 467 ± 45 Ma and 562 ± 4 Ma (compiled in Le Fort and others, 1986). Le Fort and others (1986) also obtained a Rb-Sr whole-rock isochron age of 513 ± 30 Ma from eight samples of augen-gneiss from the Higher Himalayan metamorphic belt. These indicate that the Indian continent experienced a major episode of magmatic activity around the Early Cambrian time.

The most robust sedimentary evidence for a Neoproterozoic-Cambrian orogeny have been presented from northwest Himalaya where a conspicuous angular unconformity separates the metamorphosed late Neoproterozoic (and Early Cambrian) strata from the overlying Cambrian conglomerates and sandstones (Garzanti and others, 1986; Baig and others, 1988). Garzanti and others (1986) further demonstrated a sedimentary facies transition from passive-margin carbonates to deep-water pelites with intercalated tuffites and turbidites, immediately below the above conformity in the Zanskar region of the Tethys Himalaya. This transition has been interpreted in terms of development of an arc-trench system prior to the Cambrian (-Ordovician?) orogenic uplift and shedding of molassic sediments from a foreland fold-thrust belt.

Overall, the bulk of structural, sedimentologic and geochronoloic data points to a late Neoproterozoic-Cambrian episode of deformation, metamorphism (locally migma-

tization) and syn-kinematic granitic plutonism throughout the Himalayan margin of the Indian continent. This episode which has been attributed by various authors to the Assyntian, Cadomian, late Pan-African or Hazaran orogeny in the Himalayas (Mehta, 1977; Garzanti and others, 1986; Baig and others, 1988), is consistent with the establishment of an Early Cambrian arc along the Proto-Tethyan margin of the Indian continent (fig. 12).

The Arabian Segment.—The Zagros Belt of southwestern Iran, as the extension of the Arabian platform (fig. 1) and the Mesozoic-Cenozoic subsiding passive margin of the Afro-Arabian continent, encompasses a thick cover sequence of platform sedimentary strata. Unequivocal exposures of the crystalline substratum of Zagros have not been identified. Nevertheless, the rising salt diapirs of the Early Cambrian Hormuz Formation throughout the folded Zagros and the Persian Gulf foreland basin have brought up a whole host of enclaves and exotic blocks from depth. These include a variety of igneous and metamorphic enclaves (Kent, 1979). A leucogranite enclave from the southeastern Zagros (west of Bandar Abbas, fig. 2) collected by M. Alavi, has yielded a concordant U-Pb zircon age of 547 ± 6 Ma (our unpublished data). Although this single sample by itself does not signify a magmatic arc complex, its origin, together with its association with the Hormuz Formation (equivalent of CVSU in central Iran) is suggestive of Early Cambrian magmatic activity along the length of the Arabian margin.

The Turkish Segment.—Recent Pb-Pb zircon ages (direct Pb evaporation technique) from the amphibolite-facies augen gneisses of the Menderes Massif in southwestern Turkey (Loos and Reischmann, 1995; Hetzel and Reischmann, 1996) have established approximately 560 to 530 Ma emplacement ages for the granitic precursor of these rocks. A general Precambrian age has also been proposed for the widespread, garnet-bearing mica-schists (with amphibolite and marble interlayers) in the area, based on their intrusive relationship with the augen gneisses. The bulk of geochronologic data is consistent with a major magmatic event throughout the Menderes Massif near the Precambrian-Cambrian boundary.

The weakly metamorphosed siliciclastic rocks (intercalated with diabase sills and volcaniclastic layers) of the Menderes-Taurus block in southern Turkey, known as the Bozburun sequence, share many lithostratigraphic similarities with those of the Tashk Formation in central Iran. $^{207}Pb/^{206}Pb$ ages of detrital zircon separated from the Bozburun graywackes range from 2522 ± 3 Ma to 657 ± 5 Ma (Kröner and Şengör, 1990). The unconformably overlying, fossiliferous, Middle Cambrian sedimentary strata bracket the age of this sequence between 657 Ma and approximately 533 Ma, fairly similar to those established for the Tashk Formation. Zircon from the highly mylonitized Sandikli Granite in the same area yielded Pb-Pb ages that range from 1924 ± 2 Ma to 543 ± 4 Ma, with the latter being interpreted as the age of granite intrusion (Kröner and Şengör, 1990). The Sandikli Granite thus presents a good match for the Boneh-Shurow granitic gneiss in the Saghand area.

We attribute these remarkable lithologic-age correlations to similar tectonic regimes dominating the Menderes-Taurus block and the Central Iranian Terrane in the late Neoproterozoic. They suggest that the Proto-Tethyan active continental margin might have reached as far west (south) as northern Africa (fig. 12) by the Cambrian time.

Early Cambrian Arc or Rift?

A commonly proposed model for the late Neoproterozoic-Early Cambrian (formerly Infracambrian) magmatism and sedimentation in Iran has been crustal extension associated with continental rifting (see for example, Berberian and King, 1981; Samani, 1988). It has been established that the last stages of the Neoproterozoic Pan-African orogeny in the Arabian Shield (approximately 686-517 Ma) was associated with emplacement of alkali- (A-type) granites and post-orogenic volcanics of alkaline

affinity (Brown and Jackson, 1979; Jackson and others, 1984). The Pan-African orogeny was in turn succeeded by a system of post-collisional, transcurrent faults and associated rift basins, known as the Najd system (Greenwood and others, 1976). Accordingly, the vast carbonate-evaporate deposits of the Persian Gulf and Zagros Mountains (Hormuz Formation), Oman (Ara Formation), central Iran (Rizu-Desu Series), Pakistan (Salt Range), and their correlative rocks are thought to be deposited in the rift basins of the Najd system, with the contemporaneous alkaline granites and volcanic rocks being interpreted as the products of post-orogenic, extensional magmatism (Berberian and King, 1981; Husseini, 1989). These form the basis for the suggested "syn-rift" origin of the rhyolites, felsic tuffs, and quartz-porphyries of the Rizu-Desu Series (equivalent of the CVSU) in central Iran.

Despite the above speculations, no firm evidence for the rift-drift transition, continental breakup or ocean basin formation can be found in the lower Paleozoic sedimentary (or paleomagnetic) record of the unified Arabo-Iranian platform. As an alternative scenario, Talbot and Alavi (1996) adapted an "aborted rift" tectonic model involving an (late Neoproterozoic-) Early Cambrian crust that underwent extension, but failed to drift apart, along the Arabian margin of the Gondwanaland. They too attributed the Early Cambrian magmatism to the extensional rifting of the crust and asthenospheric upwelling.

The investigated igneous and metamorphic rocks of the Saghand area and their equivalents throughout the Kashmar-Kerman Tectonic Zone sketch a tectonic history that does not corroborate the continental rift model. Regionally deformed and metamorphosed sedimentary and granitic rocks of the Boneh-Shurow complex indicate a late Neoproterozoic-Early Cambrian period of compression and lower-amphibolite facies metamorphism in an orogenic setting. The Early Cambrian granite-tonalite plutons, as well as the volcanic rhyolite-dacite associations (CVSU), demonstrably originated in an active margin environment and do not show alkaline affinities attributable to intra-plate magmatism. The late-stage, massive trondhjemite intrusions of the Saghand area provide further evidence for the Early Cambrian subduction of young oceanic crust. In summary, our geologic, geochronologic and geochemical observation in central Iran are consistent with a major episode of latest Neoproterozoic to Early Cambrian orogenic activity in an active continental-margin environment.

It must be noted that the Early Cambrian evaporite facies was only poorly developed in locations where extensive magmatic activity occurred (for example, gypsiferous horizons of CVSU in the Saghand region), thus demanding a spatial distinction between the Early Cambrian arc and the coeval salt basins. It is conceivable that the large evaporite-filled basins of the contiguous Arabia-Iran-India were developed in an Early Cambrian, extensional, back-arc environment such that parallel convergent (Proto-Tethyan) and extensional (Najd) tectonic regimes could have established along the same continental margin. The magmatic arc of the South American Andes with its back-arc zone of attenuated continental crust provides a good example for this type of setting. Undoubtedly, climate and sea-level conditions were as important a factor as structural setting in the Early Cambrian evaporite deposition.

CONCLUSION

The oldest sedimentary/volcanic successions, metamorphic rocks and magmatic intrusions exposed in the Saghand area of the Central Iranian Terrane represent the elements of a terminal Neoproterozoic-Early Cambrian magmatic arc complex. This complex belonged to a greater late Neoproterozoic-early Paleozoic orogenic system that was active along the Proto-Tethyan margin of the Gondwanaland supercontinent, extending at least from its Arabian margin to the Himalayan margin of the Indian subcontinent. Despite a possible age overlap, the Proto-Tethyan arc magmatism was

geologically distinct from, and hence unrelated to, the post-orogenic alkaline magmatism associated with the final stages of the Pan-African Orogeny in the Gondwanan interior. Therefore, the series of orogenic events that shaped the early tectonic evolution of the Central Iranian Terrane are best designated as Peri-Gondwanan or Proto-Tethyan.

At least two further episodes of orogenic activity, one in Late Triassic and another in Early Tertiary, impacted the Central Iranian Terrane prior to its final incorporation into the Alpine-Himalayan Belt. Our new geochemical and age data from the granite-tonalite intrusions of Late Triassic age in central Iran, though preliminary, bear significant implications. They corroborate the pre-existing stratigraphic and structural evidence for a Late Triassic orogenic event of probable collisional nature in the region.

The peak of Alpine orogenic activities in the Early Tertiary was evidently coeval with high-grade metamorphism and anatexis of portions of the Iranian crust (and its cover rocks), in addition to the widespread near surface magmatism. Rapid uplift and exhumation in response to continued Cenozoic continental deformation have exposed sections of the underlying metamorphosed crust in isolated fault blocks, such as those comprising the Western Domain of the Saghand region.

ACKNOWLEDGMENTS

This work constitutes for the most part J. R.'s Ph.D. dissertation. Financial support was provided by a Washington University Wheeler Fellowship and a Geological Society of America research grant to J. R., as well as a Washington University laboratory operating grant to R.D.T. INAA analyses were supported by U.S. Department of Energy grant DE-FG02-95NE38135. We thank Bob Dymek for discussions of igneous geochemistry. J. R. thanks the Geological Survey of Iran for its gracious support of his field work. Mike Williams and Edwin Gnos provided constructive reviews of the manuscript.

Appendix A

Description of the main lithostratigraphic units of the Saghand area, central Iran

Unit Name	Description	Thickness (m)	Lower Contact	Age	Age Correspondence
Boneh-Shurow Complex		Unidentified	Unidentified		
Granitic gneiss	Pink, quartzofeldspathic gneiss forming sub-parallel sheets from 20 cm to a few tens of meters thick. Characterized by a mylonitic foliation fabric of K-feldspar (microcline) and plagioclase porphyroclasts in a crystalline matrix of quartz, feldspar and micas. Epidote and biotite are common. Porphyroclasts are normally 3 mm or less in diameter. Feldspar "augen" up to 20 mm long occur in more massive gneiss varieties locally known as the Zamanabad Gneiss.			Late Neoproterozoic	Igneous emplacement
Mica-schist	Greenish-gray, strongly foliated schist interlayered predominantly with the granitic gneisses. Contains variable proportions of muscovite and biotite in a fine-grained (# 0.4 mm) granoblastic matrix of plagioclase and quartz. Biotite- or amphibole-rich layers are common. Accessory minerals include epidote, apatite, Fe-Ti oxides, zircon and, locally, garnet.			Neoproterozoic	Sedimentary deposition
Amphibolite and mafic gneiss	Dark-colored, massive amphibolite dotted with visible garnet porphyroblasts up to 25 mm in diameter. Main constituents are hornblende, plagioclase, garnet, biotite, epidote and titanite. Quartz, apatite, Fe-Ti oxides, calcite and zircon are minor or accessory minerals. Mafic gneisses contain a higher proportion of plagioclase and biotite relative to hornblende and garnet. They are lithologically transitional to the quartzofeldspathic gneisses.			Late Neoproterozoic	Metamorphism
Marble	Crest-forming, rusty to buff, coarse-grained, dolomitic marble. Locally forms interlayers or isolated lenses in alternation with the mica-schists. Interlayers range in thickness from a few meters to over 100 m. Common accessory minerals are phlogopite, tremolite, Fe-Ti oxides and apatite.			Unknown	
Mafic to intermediate (late-stage) intrusions	Mafic to intermediate dikes, sills and plugs with isotropic granular (quartz-diorite) to ophitic (diabase) textures. The common quartz-diorite consists of amphibole (hastingsite?), plagioclase and quartz with minor K-feldspar, biotite and epidote. Chilled-margins with the metamorphic country rocks are distinguishable.			Late Neoproterozoic	Igneous emplacement
Task Formation		~2000	Unidentified		
Graywacke	Fine- to medium-grained, well-bedded graywacke with dark greenish-gray colors and a weak to moderate cleavage in hand sample. Consists predominantly of detrital quartz and feldspar (# 0.5 mm in diameter) embedded in a microcrystalline (# 30 μm) matrix of quartz (and feldspars), micas and chlorite. Lithic fragments of fine-grained, quartzofeldspathic (volcanic?) aggregates and chert are abundant. Matrix biotite and chlorite represent the metamorphic constituents of the graywackes. Fine-grained, slaty varieties are common near the base of the sequence.			Unknown	
Basalt	Basaltic lava in the form of layers (flows) several meters in thickness occurs in alternation with the graywackes. Abundance and aerial distribution poorly constrained because of close outcrop similarities to the host graywackes. Studied samples from the Tashk Mountain section display relict phenocrysts of primary plagioclase and clinopyroxene, up to 2 mm in diameter, in a fine-grained groundmass of chiefly albite, biotite and epidote. Secondary (metamorphic) constituents include actinolite, chlorite, rutile and locally, serpentine and scapolite.			Unkown	
Tuffaceous rocks	Interlayers of buff, fine-grained volcaniclastic rocks up to several meters in thickness occur in close association with the basal argillaceous section of the formation. Consist of feldspar and quartz pyroclasts (up to 0.5 mm in diameter), in a fine-grained matrix of quartz and feldspar. Accessory rutile and zircon are common.			Late Neoproterozoic to Early Cambrian	Volcaniclastic deposition
Cambrian Volcano-Sedimentary Unit		~1500	Disconformity?		
Volcanic and pyroclastic rocks	Milky to greenish-white rhyolite forming flow layers several meters in thickness are most characteristic. It contains visible quartz and plagioclase phenocrysts, up to 2.5 mm in diameter, in a uniformly aphanitic and vuggy groundmass of quartz and feldspar. Phenocryst mineralogy (also chemical composition) identifies rhyodacite as the dominant rock type. Interbeds of crystal-lithic- (lapilli-) tuff containing lithic fragments of felsic volcanic type occur within the rhyodacite flows. Red-tinted, intermediate volcanic and pyroclastic rocks dominate the extrusive rocks in the Zarigan Mountain area. They include strongly silicified vitric (welded) ash-tuffs with local agglomerate interlayers and thin beds of dolomitic limestone. Subextrusive bodies of felsic rocks (*e.g.* dacite-porphyry) occur in this area, as well.			Early Cambrian	Volcanism
Carbonate rocks	Ridge-forming, light-gray to buff, dolomitic limestone with brownish weathering colors and ranging in thickness from a few meters to over 200 meters intercalate with the extrusive rocks. Internal bedding as well as lenses and nodules of chert are common. Local gypsiferous horizons have been reported particularly in the Douzakh-Darreh and Mayon Mountains (Haghipour and Pelissier, 1977).			Unknown	

APPENDIX A
(continued)

UNIT NAME	DESCRIPTION	THICKNESS (m)	LOWER CONTACT	AGE	AGE CORRESPONDENCE
Poshteh-Badam Complex		Unidentified	Unidentified	Late Neoproterozoic?	
Amphibolite and mafic gneiss	Dark-colored amphibolites and biotite-hornblende-gneisses with relict igneous textures. Consist of plagioclase, hornblende and biotite, with minor titanite and opaque minerals. Partially serpentinized ultramafic rocks (*e.g.*, pyroxenite) occur locally in close association with the amphibolites.			Unknown	
Schistose rocks	Range from carbonaceous phyllites to banded mica-schists. Consist predominantly of granoblastic quartz (and feldspar) and biotite with subordinate muscovite, opaque minerals, titanite, epidote and, locally, garnet.			Unknown	
Granitic gneiss	Uniformly medium-grained, pink gneiss with alternating bands of turbid plagioclase and granoblastic K-feldspar and quartz. Distribution uncertain because of lithologic similarities to younger granitic intrusions that intrude the complex.			Unknown	
Greenstone	Aphanitic, grayish-green greenstones dominate the complex towards north. They contain over 70% amphibole (hornblende or actinolite) with additional plagioclase, Fe-Ti oxides, biotite, epidote and titanite. Mineralogy approaches that of a pure amphibole-schist in some outcrops.			Unknown	
Marble	Foliated, fine-grained dolomitic marbles with reddish-brown weathering surfaces are intercalated with other major rock types of the complex. Distinguished from the massive marble sheets of the northern CLTD (below) based on mineralogy and superposition.			Unknown	
Marble Thrust Sheets		Unidentified	Unidentified		
Marbles	Whitish to buff, massive, uniformly crystalline marbles forming ridges, cliffs and hilltops. Separated from underlying rocks (Poshteh-Badam Complex) by low-angle (thrust) faults.			Unknown	
Chapedony Complex		Unidentified	Unidentified		
Gneiss	Massive, medium- to coarse-grained gneiss, locally porphyroblastic, with or without augen structure. Lithology ranges from a dark amphibolitic gneiss to a pink (quartzo-) feldspathic gneiss. The gray-colored augen-gneiss forms a distinct facies known as the Neybaz Gneiss. Consists of K-feldspar (up to 2 cm in diameter) and plagioclase porphyroblasts, biotite and quartz in a protomylonitic texture. Minor phases are titanite, amphibole, apatite and zircon. Pleochroic-brown allanite and myrmekitic integrowths along orthoclase margins are typical. Garnet and clinopyroxene are rare.			Eocene	Metamorphism
Migmatites	Range from millimeter-scale quartzofeldspathic seams to leucocratic veins, lenses and dikes up to several meters in thickness which locally merge to form homogeneous bodies of anatectic granite. Bands of biotite- and hornblende-rich mafic restite line the vein margins. Leucosome has a similar mineralogy to that of the Chapedony granitic gneiss (*e.g.*, abundant orthoclase) and displays a weak mylonitic fabric.			Eocene	Metamorphism and anatexis

Appendix B

Description of the dated plutonic bodies of the Saghand area, central Iran

Intrusion Name (Domain*)	Description	Contact Relationships	Age (Ma)	Magmatic Suite
Ariz Granodiorite, Polo Mountain Granodiorite (ELTD)	Pale-gray, medium-grained, composite igneous intrusions ranging in composition from tonalite (locally quartz-diorite) to granite, with granodiorite and quartz-monzodiorite as dominant lithologies. Composed of plagioclase , quartz, K-feldspar (microcline), hornblende and biotite in a hypidiomorphic-granular texture. Plagioclase laths up to 2 mm in length exhibit polysynthetic twins, oscillatory zoning and Ca-rich cores partially altered to epidote and sericite. Anhedral microcline has quadrille structure and is moderately perthitic. More felsic facies contains higher proportions of microcline and quartz relative to hornblende, biotite and plagioclase. Accessories include muscovite, epidote (allanite), titanite, zircon and Fe-Ti oxides. Opaque phases (Fe-Ti oxides) are scarce and occur only as inclusions inside biotite and hornblende. Fine-grained, amphibole-rich enclaves (mafic clots) of various sizes are common.	Intrudes the Tashk Formation. Is intruded by the Zarigan Leucogranite	533 ±1	Cambrian Granitoid Suite
Zarigan Intrusion (ELTD)			525 ±7	Cambrian Leucogranite Suite.
Leucogranite	Creamy-white to pale-gray, medium- to fine-grained, felsic intrusive rock characterized by visible, vitreous quartz in a pale-colored, groundmass of predominantly milky feldspar. Facies varies between a typical intrusive granite to a porphyritic, subextrusive rock approaching a rhyolite or granite-porphyry. Granophyric intergrowths of quartz and feldspar are common in the granite, whereas the granite-porphyry displays a distinct fabric of quartz (and feldspar) phenocrysts embedded in an aphanitic, quartzofeldspathic groundmass. Feldspar is anhedral, generally twin-free, variably turbid and is speckled with opaque (Fe-oxide?) inclusions. Polysynthetic twins are only poorly developed in some of the larger feldspars. Cross-hatched (microcline) twins are rare. Embayed (resorbed) quartz phenocrysts are common. Minor minerals include muscovite and epidote. Accessories are apatite, titanite, and zircon.	Intrudes the Tashk Formation, Cambrian Volcano-Sedimentary Unit and the Ariz Granodiorite.		
Diabase dike	Dark-colored, coarse-grained diabase with a uniform intergranular to ophitic texture, composed chiefly of plagioclase, amphibole and opaque minerals. Lath-shaped and variably epidotized plagioclase crystals up to 2 mm in length comprise nearly half of the rock. The weakly pleochroic amphibole is pseudomorphous after pyroxene. Skeletal grains of opaque Fe-Ti oxide (ilmenomagnetite) are present in significant quantities (5-10%). Accessory minerals include biotite, titanite, and zircon. Secondary epidote, chlorite, and zeolite are also present.	Gradational contacts with the host leucogranite. Dikes generally do not extend into the country rocks.		
Douzakh-Darreh Leucogranite (ELTD)	Whitish, medium-grained leucogranite characterized by a granophyric intergrowth of quartz and feldspar (mostly albite) which enclose larger phenocrysts of quartz and feldspar (mostly K-feldspar) up to 1.5 mm in diameter. Composition and facies are fairly similar to that of the Zarigan leucogranite. Visible spots of brownish leucoxene (amorphous Fe-Ti oxides and hydroxides) are relics of the primary ilmenomagnetite. Muscovite is present in small quantities, as well.	Intrudes the Tashk Formation and the Cambrian Volcano-Sedimentary Unit.	526 ±1	Cambrian Leucogranite Suite.
Sefid Granite (ELTD)	Whitish, uniformly coarse-crystalline, leucocratic granite. Consists of 10-15% plagioclase and roughly equal proportions of quartz and potassic feldspar. Plagioclase exhibits polysynthetic twins. Homogeneous potassic feldspar displays the prominent quadrille structures of microcline. Muscovite is present in variable amounts ranging from an accessory phase to about 10% of the mode. Accessories include biotite and zircon.	Intrudes the Tashk Formation.	~ 525	Cambrian Leucogranite Suite.

APPENDIX B

(continued)

INTRUSION NAME (DOMAIN*)	DESCRIPTION	CONTACT RELATIONSHIPS	AGE (Ma)	MAGMATIC SUITE
Chamgoo Granodiorite, Anarg Granodiorite (CLTD)	Medium- to coarse-grained, composite intrusion ranging in facies from a dark-gray quartz-monzodiorite to a pink, K-feldspar-rich granite. The common granodiorite variety consists of plagioclase, quartz, K-feldspar (microcline) and biotite, with subordinate amounts of allanite, epidote and muscovite. Subhedral laths of plagioclase, up to 2 mm in length, display polysynthetic twins, compositional zoning and a rather strong saussurite alteration. The anhedral microcline reaches up to 8 mm in diameter and exhibits prominent quadrille structures. It is slightly perthitic and contains abundant plagioclase (also biotite and allanite) inclusions. Myrmekitic intergrowths of quartz and plagioclase are common. Quartz has a smaller grain-size (~1 mm) and is interlocked with microcline grains of similar size in a mosaic texture. Accessory minerals include apatite and zircon.	Intrudes the Poshteh-Badam Complex.	215 ±13	Triassic Granitoid Suite
Esmailabad Granodiorite (CLTD)	Pink-colored, coarse-grained granite with a hypidiomorphic-granular texture. Consists of subhedral and strongly saussuritized plagioclase, large (up to 8 mm) perthitic microcline and quartz, with almost no primary oxides. Biotite comprises less than 10% of the mode and is variably altered to chlorite and amorphous Fe-oxide. Accessories are apatite and zircon. The grayish, plagioclase-rich facies of the pluton resembles the granodiorites of the Chamgoo intrusion.	Intrudes the Poshteh-Badam Complex and the Permian limestones. Overlain by conglomerates and sandstones of presumed Cretaceous age.	218 ±3	Triassic Granitoid Suite
Daranjir Diorite (WLTD)	Medium- to coarse-grained diorite with abundant mafic minerals, little or no quartz and locally abundant mafic enclaves. Composed of more than 50% plagioclase, together with biotite and amphibole in almost equal proportions. Euhedral to subhedral, unaltered plagioclase displays polysynthetic twins and compositional zoning. Pleochroic-green amphibole (hornblende) is closely associated with biotite. Early-stage biotite is partially overgrown by hornblende. Apatite and opaque minerals are particularly abundant in the diorite. Accessory minerals include titanite, opaques, epidote and zircon.	Is intruded by the Khoshoumi Granite. Other contacts not exposed.	43.4 ±0.2	Eocene post-metamorphic plutons.
Khoshoumi Granite (WLTD)	Coarse-grained, two-feldspar granite with abundant quartz and a considerable amount of mafic minerals. Centimeter-sized grains of pink, homogeneous, K-feldspar (orthoclase) comprise about 35% of the mode. It contains inclusions of plagioclase, quartz, biotite, and amphibole. Euhedral to subhedral plagioclase exhibits polysynthetic twins, compositional zoning and altered Ca-rich cores. Biotite and pleochroic-green hornblende account for about 10% of the mode. Accessory minerals are allanite, titanite, apatite, and zircon. Opaque oxides are rare.	Intrudes the Chapedony Complex and the Daranjir Diorite.	44.3 ±1.1	Eocene post-metamorphic plutons.

* ELTD = Eastern Lithotectonic Domain, CLTD = Central Lithotectonic Domain, WLTD = Western Lithotectonic Domain.

REFERENCES

Alavi, M., 1991, Tectonic map of the Middle East: Tehran, Geological Survey of Iran, scale 1:5,000,000.

Baig, M. S., Lawrence, R. D., and Snee, L. W., 1988, Evidence for late Precambrian to early Cambrian orogeny in northwest Himalaya, Pakistan: Geological Magazine, v. 125, p. 83–86.

Barker, F., 1979, Trondhjemite: definition, environment and hypotheses of origin, *in* Barker, F., editor, Trondhjemites, Dacites and Related Rocks: Amsterdam, Elsevier, p. 1–12.

Becker, H., Förster, H., and Soffel, H., 1973, Central Iran, a former part of Gondwanaland? Paleomagnetic evidence from Infracambrian rocks and iron ores of the Bafq area, Central Iran: Zeitschrift fuer Geophysik, v. 39, p. 953–963.

Berberian, M., 1981, Active faulting and tectonics of Iran, *in* Gupta, H. K., and Delany, F. M., editors, Zagros-Hindu Kush-Himalaya Geodynamic Evolution: American Geophysical Union Geodynamic Series, v. 3, p. 33–69.

Berberian, M., and King, G. C. P., 1981, Towards a Paleogeography and Tectonic Evolution of Iran: Canadian Journal of Earth Science, v. 18, p. 210–265.

Bowring, S. A., Grotzinger, J. P., Isachsen, C. E., Knoll, A. H., Pelechaty, S. M., and Kolosov, P., 1993, Calibrating rates of early Cambrian evolution: Science, v. 261, p. 1293–1298.

Brown, G. F., and Jackson, R. O., 1979, An overview of the geology of western Arabia, *in* Tahoun, S. A., editor, Evolution and Mineralization of the Arabian-Nubian Shield: Oxford, Pergamon Press, v. 1, p. 3–10.

Couture, R. A., and Dymek, R. F., 1996, A reexamination of absorption and enhancement effects in X-ray fluorescence trace element analysis: American Mineralogist, v. 81, p. 639–650.

Couture, R. A., Smith, M. S., and Dymek, R. F., 1993, X-Ray fluorescence analysis of silicate rocks using fused glass disk and side-window Rh source tube: Accuracy, precision, and reproducibility: Chemical Geology, v. 110, p. 315–328.

Coward, M. P., and Dietrich, D., 1989, Alpine tectonics; an overview, *in* Coward, M. P., Dietrich, D., and Park, R. G., editors, Alpine Tectonics: Geological Society Special Publications 45, p. 1–29.

Crawford, A. R., 1972, Iran, continental drift and plate tectonics: 24th International Geological Congress Report of the Session, v. 24, n. 3, p. 106–112.

——— 1977, A summary of isotopic age data for Iran, Pakistan and India: Memoire Hors Serie - Societe Geologique de France, v. 8, p. 251–260.

Davoudzadeh, M., and Schmidt, K., 1984, A review of the Mesozoic Paleogeography and Paleotectonic Evolution of Iran: Neues Jahrbuch für Geologie und Paläontologie, Abhhandlungen, v. 168, p. 182–207.

Davoudzadeh, M., Lensch, G., and Weber-Diefenbach, K., 1986, Contribution to the paleogeography, stratigraphy and tectonics of the Infracambrian and Lower Paleozoic of Iran: Neues Jahrbuch für Geologie und Paläontologie, Abhhandlungen, v. 172, p. 245–269.

Dedual, E., 1967, Zur Geologie des mittleren und unteren Karaj-Tales, Zentral-Elburz (Iran): Mitteilungen aus dem Geologischen Institut der Eidgenoessischen Technischen Hochschule und der Universitaet Zuerich, Neue Folge, v. 76, p. 123.

DeWit, M., Jeffery, M., Bergh, H., and Nicolaysen, L., 1988, Geological map of sectors of Gondwana: American Association of Petroleum Geologists, scale 1:10,000,000.

Drummond, M. S., and Defant, M. J., 1990, A model for trondhjemite-tonalite-dacite genesis and crustal growth via slab melting: Archean to modern comparisons: Journal of Geophysical Research, v. 95, p. 21,503–21,521.

Drummond, M. S., Defant, M. J., and Kepezhinskas, P. K., 1996, Petrogenesis of slab-derived trondhjemite-tonalite-dacite/adakite magmas: Transactions of the Royal Society of Edinburgh: Earth Sciences, v. 87, p. 205–215.

Förster, H., and Boroumandi, H., 1971, Jungprakambrische Magnetit-Lava und Magnetit-Tuffe aus dem Zentraliran: Die Naturwissenschaften, v. 58, p. 524–525.

Förster, H., and Jafarzadeh, A., 1994, The Bafq Mining District in Central Iran-A Highly Mineralized Infracambrian Volcanic Field: Economic Geology, v. 89, p. 1697–1721.

Garzanti, E., Casnedi, R., and Jadoul, F., 1986, Sedimentary Evidence of Cambro-Ordovician orogenic Event in the Northwestern Himalaya: Sedimentary Geology, v. 48, p. 237–265.

Greenwood, W. R., Hadley, D. G., Anderson, R. E., Fleck, R. J., and Schmidt, D. L., 1976, Late Proterozoic cratonization in southwestern Saudi Arabia: Philosophical Transactions of the Royal Society of London Series A, v. 280, p. 517–527.

Haghipour, A., ms, 1974, Etude geologique de la region de Biabanak-Bafq (Iran Central); petrologie et tectonique du socle Precambrien et de sa couverture: These, Universite Scientifique et Medicale de Grenoble, France, 403 p.

——— 1977a, Geological Map of the Biabanak-Bafq Area: Tehran, Geological Survey of Iran, scale 1:500,000.

——— 1977b, Geological Map of the Posht-e-Badam Area: Tehran, Geological Survey of Iran, scale 1:100,000.

Haghipour, A., and Aghanabati, A., 1989, Geological Map of Iran (2nd edition): Tehran, Geological Survey of Iran, scale 1:2,500,000.

Haghipour, A., and Pelissier, G., 1977, Geology of the Saghand Sector, *in* Haghipour, A., Valeh, N., Pelissier, G., and Davoudzadeh, M., editors, Explanatory Text of the Ardekan Quadrangle Map: Geological Survey of Iran, H8, p. 10–68.

Hetzel, R., and Reischmann, T., 1996, Intrusion age of Pan-African augen gneisses in the southern Menderes Massif and the age of cooling after Alpine ductile extensional deformation: Geological Magazine, v. 133, p. 565–572.

Huckriede, R., Kürsten, M., and Venzlaff, H., 1962, Zur geologie des gebiets zwischen Kerman und Saghand (Iran): Beihefte zum Geologischen Jahrbuch, v. 51, p. 197.

Hushmandzadeh, A., ms, 1969, Metamorphisme et granitisation du massif Chapedony (Iran Central): These, Universite Scientifique et Medicale de Grenoble, France, 242 p.

Husseini, M. I., 1989, Tectonic and depositional model of Late Precambrian-Cambrian Arabian and adjoining plates: American Association of Petroleum Geologists Bulletin, v. 73, p. 1117–1131.

Jackson, J., and McKenzie, D., 1984, Active tectonics of the Alpine-Himalayan Belt between western Turkey and Pakistan: Geophysical Journal of the Royal Astronomical Society, v. 77, p. 185–264.

Jackson, N. J., Walsh, J. N., and Pegram, E., 1984, Geology, geochemistry and petrogenesis of late Precambrian granitoids in the Central Hijaz Region of the Arabian Shield: Contributions to Mineralogy and Petrology, v. 87, p. 205–219.

Jäeger, E., Bhandari, A. K., and Bhanot, V. B., 1971, Rb-Sr age determination on biotites and whole rock samples from the Mandi and Chor granites, Himachal Pradesh, India: Eclogae Geologicae Helvetiae, v. 64, p. 521–527.

Jaffey, A. H., Flynn, K. F., Glendenin, L. E., Bentley, W. C., and Essling, A. M., 1971, Precision measurements of half-lives and specific activities of 235U and 238U: Physical Review C, v. 4, p. 1889–1906.

Kent, P. E., 1979, The emergent Hormuz salt plugs of southern Iran: Journal of Petroleum Geology, v. 2, p. 117–144.

Korotev, R. L., 1987, National Bureau of Standards Coal Flyash (SRM 1633a) as a multielement standard for instrumental neutron activation analysis: Journal of radioanalytical and nuclear chemistry, v. 110, p. 159–177.

——— 1991, Geochemical stratigraphy of two regolith cores from the central highlands of the moon: Proceedings of the Lunar and Planetary Science Conference, v. 21, p. 229–289.

Krogh, T. E., 1973, A low-contamination method for hydrothermal decomposition of zircon and extraction of U and Pb for isotopic age determination: Geochimica et Cosmochimica Acta, v. 37, p. 488–494.

——— 1982a, Improved accuracy of U-Pb zircon dating by selection of more concordant fractions using a high gradient magnetic separation technique: Geochimica et Cosmochimica Acta, v. 46, p. 631–635.
——— 1982b, Improved accuracy of U-Pb zircon dating by the creation of more concordant systems using air abrasion technique: Geochimica et Cosmochimica Acta, v. 46, p. 637–649.
Kröner, A., and Şengör, A. M. C., 1990, Archean and Proterozoic ancestry in late Precambrian to early Paleozoic crustal elements of southern Turkey as revealed by single-zircon dating: Geology, v. 18, p. 1186–1190.
Lawver, L. A., and Scotese, C. R., 1987, A revised reconstruction of Gondwanaland, *in* McKenzie, G. D., editor, Gondwana Six; Structure, Tectonics and Geophysics: Geophysical Monograph, v. 40, p. 17–23.
LeFort, P., Debon, F., Pecher, A., Sonet, J., and Vidal, P., 1986, The 500 Ma magmatic event in alpine southern Asia, a thermal episode at Gondwana scale: Sciences de la Terre, Memoire 47, p. 191–209.
Le Maitre, R. W., editor, 1989, A classification of igneous rocks and glossary of terms: Oxford, Blackwell, 193 p.
Lindenberg, H. G., Gröler, K., Jacobshagen, V., and Ibbeken, H., 1984, Post-Paleozoic stratigraphy, structure and orogenetic evolution of the southern Sabzevar zone and the Taknar block: Neues Jahrbuch für Geologie und Paläontologie, Abhhandlungen, v. 168, p. 287–326.
Loos, S., and Reischmann, T., 1995, Geochronological data on the southern Menderes Massif, SW Turkey, obtained by single zircon Pb evaporation: Terra Abstracts, v. 5, p. 353.
Ludwig, K. R., 1980, Calculation of uncertainties of U-Pb isotope data: Earth and Planetary Science Letters, v. 46, p. 212–220.
——— 1991, ISOPLOT: A plotting and regression program for radiogenic-isotope data (version 2.53): Reston, Virginia, U.S. Geological Survey Open-File Report, 39 p.
McKerrow, W. S., Scotese, C. R., and Brasier, M. D., 1992, Early Cambrian continental reconstructions.: Journal of the Geological Society of London, v. 149, p. 599–606.
Mehta, P. K., 1977, Rb-Sr geochronology of the Kulu-Mandi Belt: its implications for the Himalayan tectogenesis: Geologische Rundschau, v. 66, p. 156–175.
Middlemost, E. A. K., 1989, Iron oxidation ratios, norms and the classification of volcanic rocks: Chemical Geology, v. 77, p. 19–26.
Müller, R., and Walter, R., 1984, Stratigraphy, magmatism and structure of the Precambrian-Paleozoic Taknar inlier northwest of Kashmar: Neues Jahrbuch für Geologie und Paläontologie, Abhhandlungen, v. 168, p. 327–344.
PLATES Project (1999): Institute of Geophysics, University of Texas at Austin.
Powell, C. McA., Johnson, B. D., and Veevers, J. J., 1980, A revised fit of East and West Gondwanaland: Tectonophysics, v. 63, p. 13–29.
Ramezani, J., 1996, Early Cambrian tectonothermal event and basin evolution in central Iran: correlation with central and western Himalaya: Geological Society of America Abstracts with Programs, v. 28, no. 7, p. 370.
Ramezani, J., ms, 1997, Regional geology, geochronology and geochemistry of the igneous and metamorphic rock suites of the Saghand area, central Iran: Ph.D. thesis, Washington University, St. Louis, Missouri, 416 p.
Ramezani, J., Dymek, R. F., and Tucker, R. D., 1999, Trondhjemite intrusions of the terminal Neoproterozoic-Cambrian orogeny in central Iran: origin and tectonic significance: Geological Society of America Abstracts with Programs, v. 31, n. 7, p. 415.
Sahandi, M., Baumgartner, S., and Schmidt, K., 1984, Contributions to the stratigraphy and tectonics of the Zeber-Kuh Range (East Iran): Neues Jahrbuch für Geologie und Paläontologie, Abhhandlungen, v. 168, p. 346–357.
Samani, B. A., 1988, Metallogeny of the Precambrian in Iran: Precambrian Research, v. 39, p. 85–106.
Sawka, W. N., Chappell, B. W., Kistler, R. W., 1990, Granitoid compositional zoning by side-wall boundary layer differentiation; evidence from the Palisade Crest intrusive suite, central Sierra Nevada, California: Journal of Petrology, v. 31, p. 519–553.
Şengör, A. M. C., 1987, Tectonics of the Tethysides: Orogenic Collage Development in a Collisional Setting: Annual Review of Earth and Planetary Sciences, v. 15, p. 213–244.
Shand, S. J., 1943, Eruptive Rocks: London, Murby, 444 p.
Soffel, H. C., and Förster, H. G., 1981, Apparent Polar Wander Path of Central Iran and its Geotectonic Interpretation, *in* McElhinny, M. W., Khramov, A. N., Ozima, M., and Valencio, D. A., editors, Global Reconstruction and the Geomagnetic Field during the Paleozoic: Advances in Earth and Planetary Sciences 10, p. 117–136.
Stacey, J. S., and Kramers, J. D., 1975, Approximation of terrestrial lead isotope evolution by a two-stage model: Earth and Planetary Science Letters, v. 26, p. 207–221.
Stöcklin, J., 1968, Structural history and tectonics of Iran: a review: American Association of Petroleum Geologists Bulletin, v. 52, p. 1229–1258.
——— 1974, Possible Ancient Continental Margins in Iran, *in* Burk, C. A., and Drake, C. L., editors, The Geology of Continental Margins: New York, Springer Verlag, p. 873–887.
Stöcklin, J., and Setudehnia, A., 1977, Stratigraphic Lexicon of Iran (2nd edition): Tehran, Geological Survey of Iran, No. 18, 376 p.
Takin, M., 1972, Iranian geology and continental drift in the Middle East: Nature, v. 235, p. 147–150.
Talbot, C. J., and Alavi, M., 1996, The past of a future syntaxis across the Zagros, *in* Alsop, G. I., Blundell, D. J., and Davison, I., editors, Salt Tectonics: Geological Society Special Publications 100, p. 89–109.
Tucker, R. D., and McKerrow, W. S., 1995, Early Paleozoic chronology: a review in light of new U-Pb zircon ages from Newfoundland and Britain: Canadian Journal of Earth Sciences, v. 32, p. 368–379.
Unrug, R., 1997, Rodinia to Gondwana: The geodynamic map of Gondwana supercontinent assembly: GSA Today, v. 7, p. 1–6.
Valeh, N., and Haghipour, A., 1970, Geological Map of Ardekan: Tehran, Geological Survey of Iran, scale 1:250,000.